VNIVERSITAT DE VALÈNCIA

SCHOOL OF MEDICINE
DEPARTAMENT OF PEDIATRICS, OBSTETRICIS AND GINECOLOGY

ENDOMETRIAL STUDY OF A NOVEL IN VIVO EMBRYO CULTURE DEVICE

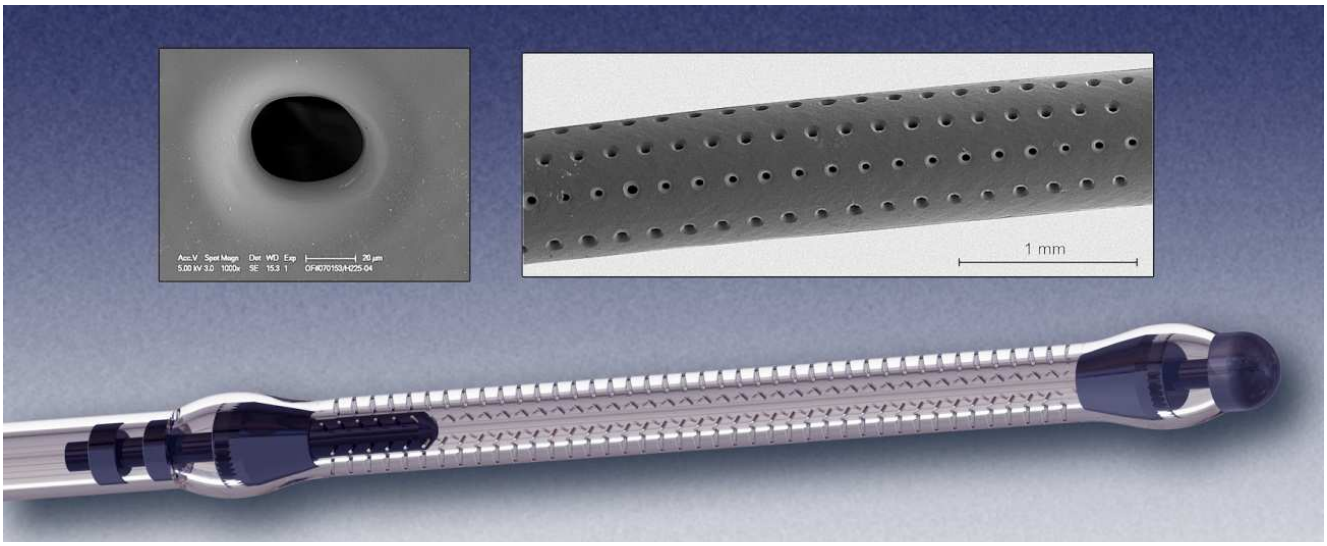

European doctoral thesis presented by:

Manuel Fernández-Sánchez

Valencia 2012

VNIVERSITAT DE VALÈNCIA

SCHOOL OF MEDICINE
DEPARTAMENT OF PEDIATRICS, OBSTETRICIS AND GINECOLOGY

ENDOMETRIAL STUDY OF A NOVEL IN VIVO EMBRYO CULTURE DEVICE

European doctoral thesis presented by:

Manuel Fernández-Sánchez

Thesis directors:

Carlos Simón Vallés

Antonio Pellicer Martínez

José Antonio Horcajadas Almansa

Valencia, 2012

D. Carlos Antonio Simón Vallés, Catedrático del Departamento de Pediatría, Obstetricia y Ginecología de Medicina de la Universidad de Valencia.

D. Antonio Pellicer Martínez, Catedrático del Departamento de Pediatría, Obstetricia y Ginecología de Medicina de la Universidad de Valencia.

D. José Antonio Horcajadas Almansa, Profesor Titular del Departamento de Biología Molecular e Ingeniería Bioquímica de la Universidad Pablo de Olavide de Sevilla.

CERTIFICAN:

Que el trabajo titulado: "Endometrial study of a novel in vivo embryo culture device" ha sido realizado íntegramente por D. Manuel Fernández Sánchez bajo nuestra supervisión. Dicho trabajo está concluido y reúne todos los requisitos para su presentación y defensa como TESIS DOCTORAL ante un tribunal.

Y para que conste así a los efectos oportunos, firmamos la presente certificación en Valencia a 20 de marzo de 2012.

Fdo. Prof C.Simór

Fdo. Prof A.Pellicer

Fdo. Prof J.A.Horcajadas

CONTENTS

1. LIST OF

ABBREVIATIONS

IVF	*In Vitro* Fertilisation
ART	Assisted Reproductive Techniques
ICSI	Intracytoplasmic Sperm Injection
ROS	Reactive Oxygen Species
IL-6	Interleukin 6
IVD	*In Vivo* Development
GIFT	Gamete Intra-Fallopian Transfer
ZIFT	Zygote Intra-Fallopian Transfer
WOI	Window of Implantation
IUD	Intrauterine Device
ER	Estrogen Receptor
PR	Progesterone Receptor
PRA	Progesterone Receptor Isoform A
PRB	Progesterone Receptor Isoform B
AF	Activation Factor
DNA	Deoxyribonucleic Acid
cDNA	Complementary DNA synthesized from a

	messenger RNA (mRNA) template in a reaction catalyzed by the enzyme reverse transcriptase and the enzyme DNA polymerase
RNA	Ribonucleic Acid
mRNA	Messenger RNA
mPR	Membrane Progesterone Receptor
miRNA	micro RNA
GPCRs	G-protein-coupled receptors
PAQR	AdipoQ Receptor
IHC	Immunohistochemistry
LIF	Leukaemia Inhibitory Factor
LIF-R	Leukaemia Inhibitory Factor Receptor
LEPR	Leptin Receptor
PCR	Polymerase Chain Reaction
RT-PCR	Reverse transcriptase PCR
EECs	Endometrial Epithelial Cells
ESC	Endometrial Stromal Cells

PKs/PROKs	Prokineticins
EG-VEGF	Endocrine Gland-Derived Vascular Endothelial Growth Factor
PCOS	Polycystic Ovarian Syndrome
Bv8	Bombina variegata 8
PROK-R1	Prokineticin Receptor 1
PROK-R2	Prokineticin Receptor 2
IP3	Inositol Phosphate 3
COX	Cyclooxygenase
hCG	Human Chorionic Gonadotropin
DKK1	Dickkopf 1
WNT	Family of Signalling Secreted Lipid-Modified Proteins. The origin of the name Wnt comes from a hybrid of Int and Wg (wingless) in *Drosophila*, which is the best characterized Wnt gene
FSH	Follicle Stimulating Hormone
rFSH	Recombinant Follicle Stimulating Hormone

LH	Luteinising Hormone
GnRH	Gonadotrophin-Releasing Hormone
OCP	Oral Contraceptive Pill
CO2	Carbon Dioxide
DAVID	Database for Annotation, Visualization and Integrated Discovery
STRING	Search Tool for the Retrieval of Interacting Genes/Proteins
PCA	Principal Component Analysis
NSAIDs	Non-Steroidal Anti-Inflammatory Drugs
ABC	Avidin - Biotin Immunohistochemistry Method
Ig	Immunoglobulin
LSAB	Labelled Streptavidin-Biotin

2. INTRODUCTION

Since Louise Brown, the first IVF (in vitro fertilisation) baby born in 1978 [1], assisted reproductive techniques (ARTs) have become commonplace. It is estimated that 1-4% of the population in developed countries was conceived using this technology [2]. In 2008 alone, 148,055 ART cycles were performed in 436 reporting clinics in the USA, resulting in 46,326 live births, corresponding to over 1% of all infants born in the USA [3]. According to the European Society of Human Reproduction and Embryology (ESHRE), within Europe, the countries with the most reported ART cycles were France (66,000), Germany (55,000), Spain (50,000), the UK (44,000) and Italy (41,000). In Spain, 106 out of 160 clinics reported a total of 55,134 cycles of IVF/ICSI in 2009 [4] and the largest number of egg donation cycles of any country in Europe [5].

2.1 "*In Vitro*" EMBRYO DEVELOPMENT

Knowledge about embryonic development inside *(in vivo)* and outside *(in vitro)* the physiological environment of the reproductive tract and endometrial receptivity is increasing. However, more research is needed on several topics, such as the dialogue between the embryo and endometrium, early embryo development and a wide variety of relevant actions that are required to accomplish the objective of every infertility treatment: a healthy baby.

Preimplantational development is a process involving many important steps, such as oocyte maturation, cleavage divisions, embryonic genome

activation, compactation, blastocyst formation, expansion, hatching and implantation into the endometrium [6].

A receptive endometrium is mandatory for implantation to occur [7], and embryonic implantation has classically been divided into three consecutive phases: apposition, adhesion and invasion. During apposition, the human blastocysts find a specific area in the maternal endometrium in which to implant. In the adhesion phase, which occurs 6-7 days after ovulation within the “implantation window”, direct contact occurs between the endometrial epithelium and the trophectoderm. Finally, in the invasion phase, the embryonic trophoblast traverses the basement membrane, passes the endometrial stroma and reaches the uterine vessels [8]. Successful implantation requires both synchronous embryonic development and an interaction between blastocyst and endometrium. Regulation of molecules such as the integrins promotes blastocyst adhesion [9]. The molecular mechanisms regulating embryo implantation have been studied using decidualization and knock-out (KO) mouse models identifying genes that are functionally involved in endometrial receptivity.

In ARTs, fertilisation occurs outside of the Fallopian tube, and the preimplantation embryos are cultured in vitro before being transferred into the uterus. Therefore, embryo quality varies widely both between and within patients.

The embryo is able to develop in the in vitro culture medium and has the ability to adapt to environment changes to a certain extent. If

environmental changes exceed this capacity to adapt, abnormal embryonic development may result [10].

The effect of culture conditions on the embryonic epigenetic program has been investigated in the mouse model by comparing the imprinting status of in vivo versus in vitro cultured embryos using five different commercial media [11]. Embryos were analysed for H19, Snrpn and Peg3, demonstrating that in vivo-derived embryos were superior to all five culture systems in terms of genomic imprinting.

However, a related study did not find significant differences between in vivo and in vitro developed blastocysts [12]. In contrast to the Market-Velker study, in which pools of five blastocysts were used for the imprinted methylation analysis, this team derived stem cells (ES) from both in vivo and in vitro embryos. They observed that in vitro stem cells had increased abnormal genomic imprinting compared with in vivo stem cells, but only at early passages [12]. At later passages, they did not observe significant differences.

New developments give us some information about the incorporation of specific amino acids into the medium to prevent metabolic changes [13] and to favour the development of a new generation of sequential embryo culture media that have dramatically increased the ART success rate [14], except in aging patients [15].

Non-invasive methods have been developed as alternatives to

aneuploidy screening, such as metabolic profiling based on the analysis of embryo culture media [16]. In this approach, the comparison of the aneuploidy levels of six chromosomes related to early pregnancy loss with the amino acid metabolism profile of day 2 to 5 embryos demonstrated that abnormal embryos presented altered amino acid turnover in vitro compared with their normal counterparts [17].

A frequent feature of in vitro culture is that cleaved embryos arrest their development at the 2- to 4-cell stage [18]. A great deal of research has attempted to elucidate possible causes and mechanisms of this phenomenon. Embryos cultured in 20% oxygen conditions display significantly elevated levels of intracellular reactive oxygen species (ROS) and higher frequencies of permanent embryo arrest compared with the embryos produced under 5% oxygen atmospheres [19]. Although this finding seems to imply that low-oxygen and antioxidant treatments can improve embryo development, the problem of oxidative stress is far more complicated (for review, see Betts and Madan in 2008 [20]).

Embryologists have always used morphological criteria to identify the most viable embryo [21]. New strategies being explored include proteomic and metabolomic profiling [22, 23], birefringence imaging [24], oxygen consumption [25] and time-lapse imaging [26]. Another tool for embryo selection is to examine the oxidative status of the embryo [27].

Co-culture system

To enhance in vitro development, embryos have been cultured in the presence of nursing cell types, developing coculture systems. In 1965, Cole and Paul managed to co-culture mouse embryos with irradiated HeLa cells [28]. Later, Allen and Wright co-cultured porcine embryos at various stages of development on porcine endometrial cell monolayers [29]. Since then, this strategy has been used in bovine [30] and human embryos [31] at the clinical level to improve blastocyst number and quality in patients who have suffered implantation failure in an oocyte donation program, but not in IVF patients [32]. The five-year (1997-2001) clinical experience in blastocyst transfer cultured on heterologous endometrial epithelial cells as co-culture systems in our group revealed an increase of blastocyst formation rates and an improvement in implantation and pregnancy rates [33].

Non-invasive diagnosis

The secretome profile of implanted blastocysts grown in sequential versus endometrial epithelial cell co-culture systems has been analysed, demonstrating that more IL-6 was consumed in the media of viable embryos compared with blastocysts that did not implant. This finding supports the idea that IL-6 could be important for embryo development and viability [34].

Currently, there is a trend to optimise costs/benefits by going back to more physiological treatments. The use of mild ovarian stimulation [35] and single embryo transfer [36] are just two examples. In vivo embryo culture is

another option that would also contribute to advancing the state of the art.

Thus, developing new in vivo embryo development techniques without disrupting the embryo-endometrial dialogue would be of great interest for the future of ART.

2.2 "*In vivo*" EMBRYO DEVELOPMENT

An in vivo culture system exists inside the uterine cavity in an in vivo development (IVD) system. IVD is a wise alternative to the in vitro culture system, with the expected physiological merits of a natural microenvironment. The use of cell encapsulation allows control of the culture duration and convenient retrieval of embryos for diagnosis prior to leaving them to implant within the uterine endometrial wall.

The medical device developed by ANECOVA SA (product family: Anecova-d1; Device reference: ACVd1) has been classified as Class II by the notified body (CE Mark). This device consists of three main parts: the capsule (vessel for the gametes), the connection system (stabilisation) and the retrieval string.

A first prototype was used in the present clinical investigation to demonstrate that the device was capable of being introduced through the cervix, immobilised at the desired location for a specific period of time (up to 6 days) and retrieved easily.

To ensure relevant biocompatibility of this device towards the gametes

(oocytes, sperm) and embryos, Anecova carried out an in vitro toxicity test using mouse and bovine embryos. The results of these tests provided evidence that the components and materials used in the device were non-toxic for bovine embryos and biologically neutral in terms of fertilisation and embryonic development.

This study also provided evidence that the device could be safely and accurately loaded and unloaded with bovine embryos that have an equivalent size to human embryos at the same development stage. Moreover, every material and the device itself were tested in vitro using a mouse embryo model.

2.3 ENDOMETRIAL RECEPTIVITY

The endometrial tissue consists of an inner lumen that is lined with an epithelial cell layer from which emerge glandular structures that are also lined by epithelial cells. Glands produce embryonic factors that are essential for the embryo to attach and invade the stromal compartment to establish the pregnancy.

Endometrial receptivity is acquired during a short period of time in the mid-luteal phase referred to as the window of implantation (WOI) defined by timing to the LH surge. During this period of time (LH+7 to LH+9), the endometrial epithelium acquires a functional ability to support blastocyst adhesion [37]. Stromal cells differentiate into decidual cells after LH-9 to support trophoblast invasion and placental development.

To explain the basic mechanisms implicated in endometrial receptivity, researchers have investigated the morphological changes and modifications of the plasma membrane [38] and cytoskeleton [39] using histology, electron microscopy, molecular biology and biochemistry in animal models and humans.

In the pregenomic era, the single-molecule approach was a useful way to investigate candidates for endometrial receptivity. Among the main factors identified are leukaemia inhibitory factor (LIF), leptin and integrins, although none of them has proven to be clinically useful as biomarkers [40].

Leptin is an adipocyte-specific hormone that regulates adipose-tissue mass through hypothalamic effects on satiety and energy expenditure, acting through the leptin receptor (LEPR), a single-transmembrane-domain receptor of the cytokine receptor family [41]. Depending on the intracytoplasmic domains, at least six leptin receptor isoforms (Ob-Ra, b, c, d, e, and f) have been described from different RNA splicing [42]. Ob-R knockout mice are obese and infertile, and this phenotype can be restored by exogenous leptin treatment, but not by food restriction [43]. Leptin and OB-Rt mRNA has been identified in human oocytes and preimplantation embryos at different stages (oocyte metaphase II, two-cell, four-cell, eight-cell, morula, expanded blastocyst and hatched blastocyst) [44] and in the human endometrium [45].

LIF binds to a heterodimeric receptor that consists of two transmembrane proteins: LIF receptor (LIF-R) and gp130 [46], a common receptor for IL-6 family cytokines. LIF-knockout mice are infertile

because of the lack of embryonic adhesion, which can be restored by exogenous LIF. LIF-/- embryos implant normally in the uteri of wild-type recipients, indicating the importance of this cytokine for mouse implantation [47].

A crucial process in the cyclical tissue regeneration and growth of the normal endometrium is angiogenesis regulated in part by prokineticins (PKs). PKs are a recently discovered family of angiogenic factors [48] formed by PK1/PROK-1, also known as endocrine gland-derived vascular endothelial growth factor (EG-VEGF), and PK2/PROK-2, also known as Bv8 (Bombina variegata 8).

PROK-1 induces proliferation, migration, and fenestration in capillary endothelial cells. Its expression is similar to VEGF, induced by hypoxia and restricted to steroidogenic organs (ovary, testis, adrenal, and placenta). PROK-2 expression shows a similar distribution, but with stronger expression in the testis and leukocytes [49, 50].

Prokineticins bind to two closely related G-protein coupled receptors, known as prokineticin receptor 1 (PROK-R1) and prokineticin receptor 2 (PROK-R2), both of which are able to bind PROK-1 and PROK-2 with similar affinities [51].

In the human endometrium, the expression of PROK-1 and its receptor has been reported using quantitative RT-PCR. Furthermore, PROK-1 and PROK-2 were localised by immunohistochemistry and in situ hybridisation to

various endometrial components [52] with high expression of PROK-1 in the secretory phase while PROK-2 is quite stable.

Evans' team elucidated the manner in which the interaction between PROK-1 and PROK-R1 regulates the expression of other factors related to decidual response, such as COX-2. This factor is a key regulator of prostaglandin synthesis. Substantial evidence has suggested that COX-2 is expressed in cells that are known to participate in inflammatory conditions [53]. Evans and colleagues reported that PROK-R1 and COX-2 colocalise to glandular epithelial and stromal cells of mid-secretory endometrium and first-trimester decidua. According to their results, PROK-1 may have a great ability to regulate COX-2 expression in both compartments during endometrial receptivity and early pregnancy. A new signalling pathway triggered by hCG has been suggested that induces both PROK-1 and LIF expression and mediates maternal-embryonic crosstalk [54]. Recent publications have found a correlation between genetic polymorphisms in PROK-1 and PROK-R1 and recurrent miscarriage [55] and have also associated a defective decidualization process and recurrent miscarriage with an aberrant elevation in PROK-1 expression [56].

PROK-1 and Dickkopf 1 (DKK1) have been investigated during the period of endometrial receptivity and early pregnancy, demonstrating that both genes regulate endometrial actions, such as epithelial cellular proliferation and differentiation of the stroma during early pregnancy [57]. DKK1 is a secreted protein with two cysteine-rich regions and is involved in

embryonic development through the inhibition of the WNT signalling pathway.

In the genomic era, numerous studies have investigated the gene expression profile of the human endometrium [58]. These analyses have generated long lists of candidate endometrial receptivity genes [59]. Accumulated evidence indicates the presence and function of estrogen and progesterone receptors in stromal and epithelial compartments [60, 61]. The estrogen receptors (ER) are found in all endometrial cell types, whereas progesterone receptor (PR) expression varies depending on the cell type and phase of the ovarian cycle.

The actions of steroid receptors are clearly influenced by specific coactivators and corepressors that mediate steroid hormone action. Lessey and collaborators suggested that the overexpression of one or more p160 coactivators induces the endometrium to become more sensitive to estrogen and that such overexpression may thus account for the higher incidence of endometrial abnormalities seen in women with PCOS [62].

Progesterone plays a crucial role in the reproductive process associated with the initiation and maintenance of pregnancy. Many genes that are regulated and affected by progesterone are likely to be involved in both activation and repression during the secretory phase.

PR, a member of the steroid receptor superfamily, mediates the physiological effects of progesterone. Some research on selective

progesterone receptor modulators has demonstrated that the mechanisms of action and the effects of these receptors on tissues of the reproductive system have potential efficacy for gynaecologic indications [63].

The published research prompted us to support the idea that PR is critical for embryo implantation [64]. The *PR* gene uses separated (ER)-inducible promoters and translational start sites to produce two different isoforms, PRA and PRB, which are identical except for an additional string of 165 amino acids that is present only in the N terminus of PRB [65]. This region, which is unique to PRB, contains a third transcription activation factor (AF3) in addition to the two other activation factors, AF1 and AF2, that are common to both PRA and PRB [66].

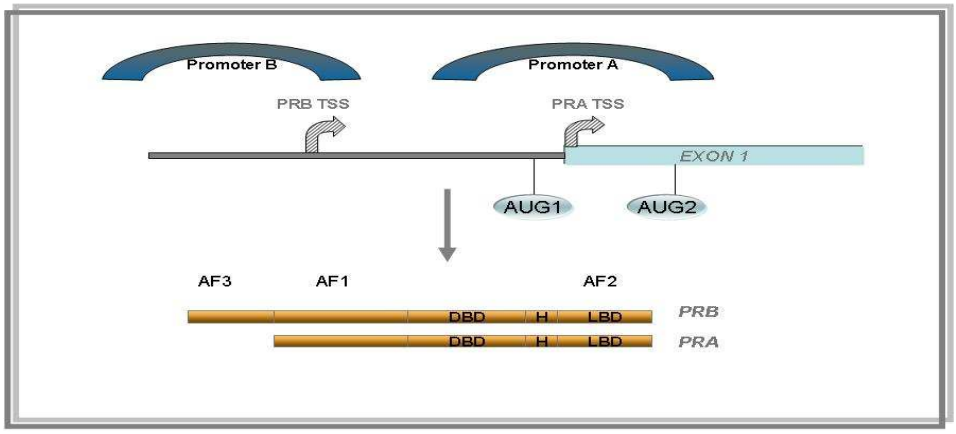

Figure 1: Scheme of PRA and PRB promoters. There are two alternative transcription starting sites (PRB TSS and PRA TSS). Two alternative translational initiation sites for PRB and PRA are shown as AUG1 and AUG2, respectively. DBD: DNA binding domain; H: hinge domain; and LBD: ligand binding domain. AF1, AF2 and AF3 are transcription activation factors.

Progesterone crosses the nuclear membrane to bind directly to PR located in the nucleus. The activated PR moves into nuclear aggregates, or 'foci', whereas unbounded PR is distributed evenly throughout the nucleus [67]. In human tissues, ligand-dependent dimerisation between PRA and PRB is required to form the functional transcription factor unit on DNA.

Although PRA and PRB are distinct transcription factors that mediate different responsive genes and physiological effects, they share several structural domains. PRB is considered a strong activator of transcription of several PR-dependent promoters in a variety of cell types in which PRA is inactive.

Both PRA and PRB are stimulated in the human endometrium by the presence of estrogen during the follicular phase, and their expressions are maximal around ovulation. On the contrary, PR expression diminishes as the P levels increase during the secretory phase [68].

Although the in vivo evidence is very weak, several transfection experiments have shown that PRA can act as a dominant negative inhibitor of PRB, dependent upon cell type and promoter context [69]. Moreover, PRA, but not PRB, is critical for endometrial function, including embryo implantation and decidualisation, in PR knockout mice [70].

The binding of P results in the formation of active PR homodimers and heterodimers between receptor isoforms. Conneely and colleagues published a study in which they generated a PRB knockout model [71], confirming that

selective activation of PRA by progestin agonists is sufficient to mediate the ovulatory activities of progesterone and that heterodimer interaction with PRB is not required for this event. However, the disruption of the normal expression pattern of PRA may lead to aberrant regulation of proliferative target genes in the mammary gland. These researchers suggested that selective activation of PRA using isoform-selective agonists could have a protective effect against both uterine and mammary gland hyperplasias.

Both investigations suggested that PRA is the predominant isoform expressed in the female reproductive tract and mammary glands in the mouse. However, the results cannot be straightforwardly extrapolated to humans.

In human endometrium, PRA and PRB have been co-localised by single cell analysis [72]. There is homogeneous expression of the two isoforms in the nuclei within the same tissue compartment during most of the phases of the menstrual cycle, with some exceptions. A predominance of PRB exists in the glands in the mid-secretory phase of the cycle, suggesting that estrogen binding to ER in the glands may cause this increase. In the secretory phase, the dynamics of PRB in the stroma were similar to those described in the glands, except that the magnitude of the changes was less pronounced.

Thus, the discordance of progesterone down-regulation of these receptors in the glandular epithelium suggests differential sensitivities of the two isoforms to the effects of progesterone during the secretory phase.

PRs distribute into specific nuclear foci under hormonal control in normal human endometrium during the menstrual cycle [67]. Both receptors were less evenly distributed and localised in discrete subnuclear foci during the mid-secretory phase compared with the proliferative phase and early secretory phase. Researchers also showed an increase in the number of PRB into nuclear foci compared with PRA at all stages of the menstrual cycle. This finding suggests that PRB may have more transcriptional activity than PRA. Mote's [72] data on the predominance of PRB expression in the glandular epithelium during the mid-secretory phase, combined with the findings in this study, suggest that PRB could be the principal mediator in the human uterus.

Given that PRA and PRB are expressed in most human tissues, variations in the expression levels of specific PR co-regulators, which have different affinities for the PR, likely support a mechanism by which a functional prevalence of PRA and PRB is managed.

Although these nuclear receptors mediate the majority of progesterone's actions, other progesterone receptors situated in the cell membrane have been documented in teleost fish [73] and subsequently in mammals [74]. These receptors are a potential mediator of non-traditional progestin actions, particularly in tissues where PR is absent. There are three membrane-PR gene isoforms, mPRα (PAQR VII), mPRβ (PAQR VIII), and mPRγ (PAQR V), whose mechanism of action begins quickly with the binding of the progestin, the activation of G proteins and their downstream signalling

pathways.

Two additional related proteins named mPRδ and mPRε have also been shown to bind progesterone. These receptors have no apparent homologies with known G-protein-coupled receptors (GPCRs) or nuclear progesterone receptors. They belong to the adiponectin receptors of the progesterone and adipoQ receptor (PAQR) family [75]. MPR isoforms' functionality has been implicated in oocyte growth [76], transport [77] and the preparation of the uterus for implantation, gestation, foetal development [78] and parturition [79].

IUDs

IUDs represent one of the most effective contraception methods because they induce changes causing endometrial refractoriness that prevent embryonic implantation [80]. The forerunners of the modern IUD were small stem pessaries used in the 1800s: small button-like structures that covered the opening of the cervix and were attached to stems extending into the cervical canal [81].

In 1902, a device that extended into the uterine cavity was developed by Hollweg in Germany and used for contraception. It was sold for self-insertion, but the risk of infection was great, earning the condemnation of the medical community [82].

Surprisingly, doctors did not begin to understand and use IUDs until the 1960s. The foreign body, now made of metal or plastic, is treated

as a foreign element and is attacked by the immune system. In the 1960s and 1970s, a plethora of types were introduced. The devices developed were made of plastic (polyethylene) impregnated with barium sulphate so that they would be visible on an x-ray, such as the Lippes Loop, which quickly became the most widely prescribed IUD in the United States in the 1970s [83].

The addition of copper to the IUD was proposed by Zipprt, whose experiments with metals indicated that copper had local effects in the endometrium [84]. Studies also indicate that copper acts as a spermicide and could reduce the motility of spermatozoids and their capacity to fertilise [85]. The copper IUD is associated with an inflammatory response marked by an influx of polymorphonuclear leukocytes, mast cells and macrophages [86]. It has been postulated that this inflammatory process creates an unsuitable environment for the embryo.

The impact of IUDs on endometrial molecules such as integrins at the time of implantation in fertile women has been demonstrated [87]. Moreover, a differential expression pattern of HOXA10 has been documented in response to copper-IUD use [88].

Our group has investigated the effect of an inert intrauterine device on the endometrial gene expression profile using microarray technology. The majority of genes altered during the refractory endometrium remained dysregulated two months after IUD removal. However, one year later, most of

them returned to a normal level of gene expression [89].

This evidence demonstrated the importance of investigating whether the Anecova device induces an endometrial refractory alteration in genomic or proteomic terms similar to those exerted by common IUDs.

3. OBJECTIVE

The present work was conducted at the IVI Valencia and at the Queen's Medical Research Institute in Edinburgh to investigate whether the Anecova device inserted in the lower segment of the endometrial cavity affects endometrial receptivity.

The first objective of the study was to evaluate the clinical impact of this IVD system in the maternal endometrium. For this purpose, we tested the endometrial effects of an unloaded device (i.e., the capsule was not loaded with gametes or embryos) for a period of up to 6 days. The evaluation was focused on verifying device tolerance by a daily clinical evaluation and direct observation through hysteroscopy after the device's retrieval.

The second aim was to evaluate whether the presence of the device causes any change in the endometrial receptivity genomic profile. For this reason, using a wide genomic approach, we analysed the gene expression profile of the endometrium obtained at day hCG+7 from ovum donors undergoing IVF in whom this device was inserted for one, three or five days compared with the same woman's endometrium without the device. Gene expression changes induced by an inert IUD were used as a control.

Both studies were conducted in accordance with the requirements of European Standard EN 540 (1993).

4. MATERIALS AND METHODS

4.1PATIENTS, INFORMED CONSENT AND INSTITUTIONAL REVIEW BOARD APPROVAL

The study was carried out at the Instituto Valenciano de Infertilidad (IVI), Valencia (Spain). Patients from the IVI ovum donation programme volunteered to participate in this clinical study. They were informed about their participation in this project and signed an informed consent form. This study was financed by Anecova and was approved by the IVI's Ethical Committee on July 29, 2004. The research number for this clinical trial is NCVPTRV1.

4.2 MEDICAL DEVICE

Two different prototypes of a new intrauterine device were developed by Anecova (ANECOVA S.A., Geneva, Switzerland) and used for this project.

Model "F": ACVd1-F is used as a product reference for devices without stabilisation. We used this model for the study of clinical security and stability of the device. It is composed of a distal titanium cap, embryo capsule, proximal titanium cap, silicon connector, intracervical stabiliser, reinforcement spring and a suture (Fig. 2).

Model "S": ACVd1-S is used as a product reference for devices with intra-cervical stabilisation. This model was used to analyze gene expression with microarray technology. It consists of a distal titanium cap, proximal titanium cap, silicon connector, intrauterine stabiliser, suture, bumper,

stabiliser sheath and intracervical sheath (Fig. 3).

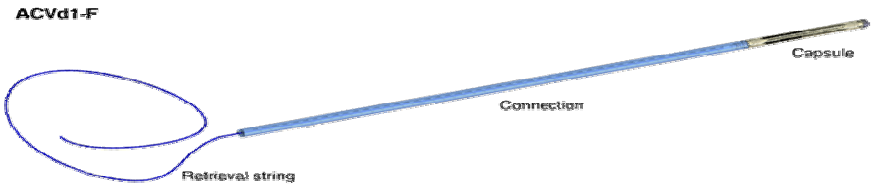

Figure 2: Model ACVd1-F Anecova device.

Figure 3: Model ACVd-S Anecova device.

The device was inserted into a standard embryo catheter provided by Anecova S.A by using transvaginal ultrasound. The embryologist first uses a placer wire to introduce the device into the catheter. Then, we use the wire to keep the device correctly located in the uterus while the catheter is removed from the uterine cavity.

Plastic sterile tweezers provide by Anecova are used for both the assembly and disassembly of the device. Any manipulation was accomplished with these tweezers inside a vertical flow cabin.

4.3 STUDY DESIGN

The women included in the study were volunteers from the ovum donation program aged 18 to 35 years without a history of hereditary diseases, predisposition to infection, or gynaecological disease such as endometriosis, polycystic ovary syndrome or hydrosalpinx. All women with known disease incompatible with clinical investigation, such as pelvic inflammatory disease, and patients with usual activity incompatible with this study, such as job schedules that do not allow time to go to medical visits, were excluded.

For the first set of clinical experiments testing safety and stability, eleven volunteers were recruited. Two of them were excluded because one refused to participate and another could not be contacted. Thus, a total of nine patients participated in this part of the study.

All patients were informed of the potential risks and burdens of the present clinical investigation prior to participating, such as the need to limit physical activities; irritation of the uterus, cervix or vagina; pain or bleeding; and infection (in the case of a sterility defect in the device and/or ancillary).

The Anecova device was inserted immediately after oocyte retrieval and removed after 24 hours in five patients (Group 1) and after 6 days in the other three (Group 2). In one patient, the device was expelled before removal. Transvaginal ultrasound was performed every day of the device's insertion. A diagnostic hysteroscopy was performed the day after the extraction of the

device. A questionnaire was given after the first ultrasound scan. Patients enrolled in Group 1 were prescribed bed rest during the test period.

Because the volunteers were ovum donors, none of them had embryo transfer, and the endometrial effects of the device could be investigated.

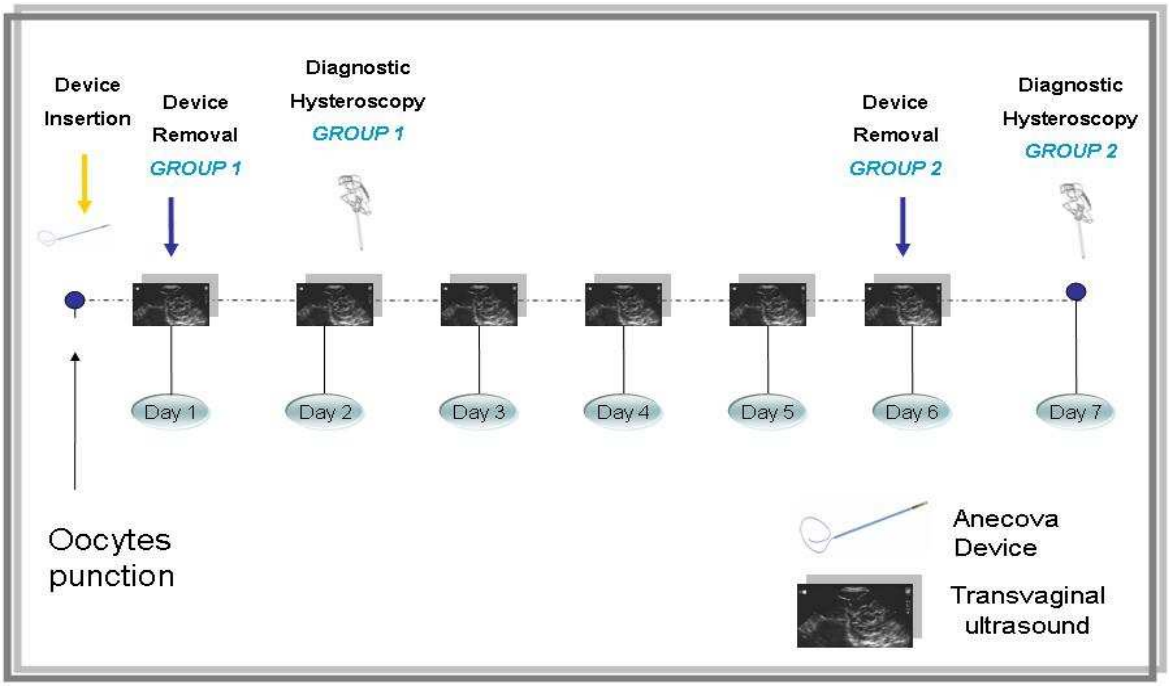

Figure 4: Schematic of the study design for clinical investigation.

Second, the molecular study of the impact of the Anecova device on the endometrium was performed using a wide genomic approach in 20 ovum donors at day hCG +7. Patients were allocated into 4 groups (n=5 per group), in which the Anecova device was inserted for 18 hours, 3 days or 5 days after oocyte retrieval and then removed. The control group was composed of endometrial samples from ovum donors in whom the device was not inserted (Fig. 5). All patients underwent a routine stimulation protocol, and

endometrial biopsy was performed at hCG+7.

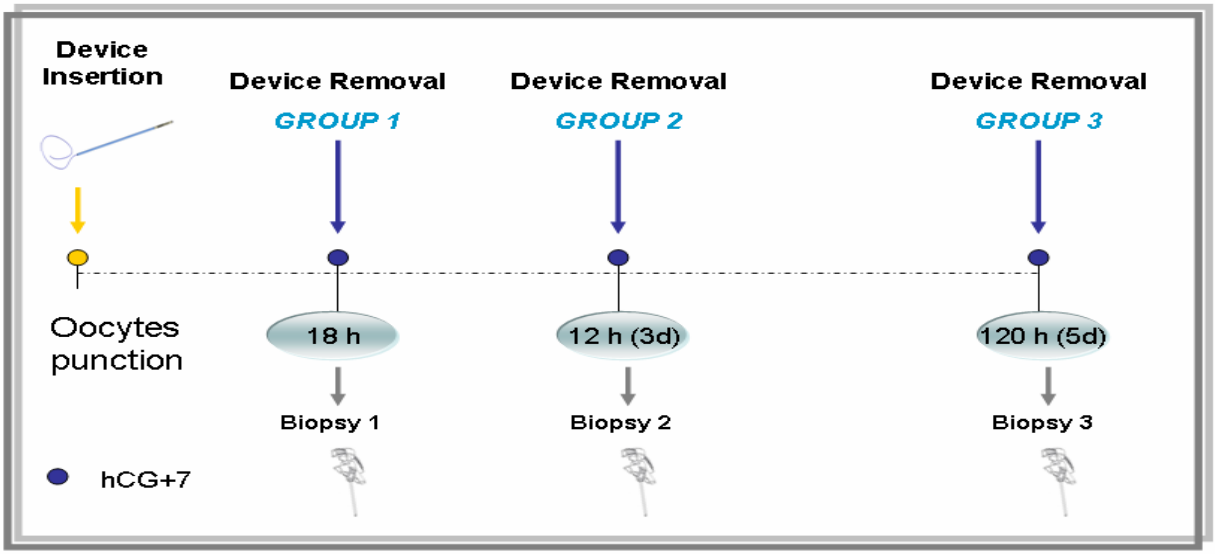

Figure 5: Schematic of the study design for the endometrial study

Finally, as an additional control, we decided to investigate the expression of key molecules for endometrial receptivity at the immunoreactive protein level in IUD users. We analysed the staining of progesterone receptors (PRA and PRB), prokineticin 1 (PROK-1), prokineticin 1 receptor (PROK-R1) and leukaemia inhibitory factor (LIF).

This study was approved by the ethics committee of the institutions where the endometrial biopsies were obtained (Génesis Unidad de Fertilidad y Reproducción, Caracas, Venezuela) and processed (Instituto Valenciano de Infertilidad, Valencia, Spain). Endometrial samples were obtained after written consent from patients. The clinical and laboratory work was performed at the Instituto Valenciano de Infertilidad and at the Queen's Medical Research Institute, University of Edinburgh, United Kingdom.

Endometrial samples from three healthy, fertile volunteers (aged 23–39 years, with a body mass index between 19 and 25 kg/m^2) were obtained at LH+7 in month 1 during a natural cycle before IUD insertion; in month 2, the IUD was inserted; in month 3, the IUD was removed, and an endometrial sample was collected immediately after IUD removal; and a final sample was obtained at month 15. Therefore, endometrial biopsies were obtained at months 1, 3 and 15 in each woman at LH+7 as determined by assaying the LH surge in serum (Fig. 6).

Overall, 10 biopsies (n=3 at months 1, 3 and 15, respectively (2 biopsies from the patient A at month 15)) were obtained using a Pipelle catheter (Genetics, Namont-Achel, Belgium) under sterile conditions from the uterine fundus. Endometrial dating was performed using the Noyes criteria [90]. The inert IUD used in this study (Lippes Loop Intrauterine Double-S; Ortho Pharmaceutical Corp, Raritan, NJ) was chosen because it contains no hormones.

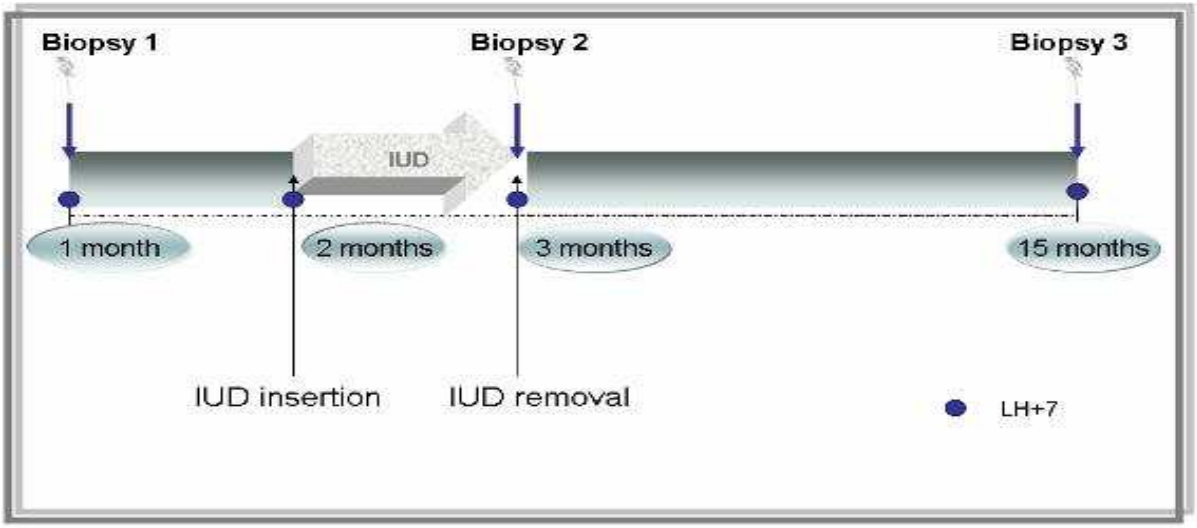

Figure 6: Schematic of the study design and tissue collection schedule

4.4 CLINICAL PROCEDURE

4.4.1 Ovarian Stimulation Protocol

Recombinant FSH (rFSH) (Puregon, Organon) and GnRH antagonist Ganirelix (Orgalutran, Organon) were used for ovarian stimulation. In summary, a low-dose, monophasic-combined oral contraceptive pill (OCP) containing 150 mg of desogestrel and 30 mg of ethinylestradiol (Marvelon, Organon) was administered for 2 weeks starting on Day 1 of the pre-ART cycle. rFSH at a dose of 200 IU per day was started 5 days after discontinuation of the OCP. Ganirelix was initiated at a daily dose of 0.25 mg on Day 6 of the rFSH stimulation. Oocyte maturation was induced by the administration of 10,000 IU of hCG (Lepori 2500 UI 4 vials) when at least three follicles ≥17 mm diameter were present on ultrasound scan. Oocyte retrieval was carried out 36 h after hCG Lepori injection by vaginal ultrasound-guided puncture of ovarian follicles.

4.4.2 Hysteroscopy

For this study, a diagnostic hysteroscopy was performed on the day of the extraction of the device with a rigid 30-degree telescope whose outer diameter is 2, 9 mm. We used a telescope with a length of 30 cm (Kark Storz Endoscopy, Tuttlingen, Germany).

The 30-degree telescope permitted rapid, dextrous evaluation of the anterior walls, posterior walls, and cornual recesses. Simply rotating the

telescope slightly to the right or left allowed a view of the tubal ostia. In comparison, the same view with a 0-degree scope requires angling the instrument to the left or right.

The video system consisted of a TV monitor with S-VIDEO output (Sony LMD 2010 LCD), single-chip endoscopic video camera (Telecam SL, Karl Storz), and a camera control unit (Telecam SL, Karl Storz).

To provide reasonable clearance for a 2, 9-mm telescope, we used a diagnostic sheet with an outer diameter (OD) of 4, 3 mm (Bettochi; Karl Storz).

Our design consisted of a hollow tube, usually fitted with two stopcocks (right and left) for the installation of the distending medium. An operating channel mounted on the posterior or anterior surface and fitted with a stopcock feeds into the common channel (Luer-Lock, Karl Storz). The light source used was a light generator and a transmitting fiberoptic cable (Xenon NOVA 175 Karl Storz). It is usually called Cool Light because the infrared rays have been omitted from the light spectrum to prevent a warming effect. Hysteroscopy material was sterilised by autoclave.

Distension was accomplished by insufflation with carbon dioxide (CO2) gas or by instillation of an electrolytic or non-electrolytic fluid. Fluids can be used for both diagnostic and operative procedures. Although CO2 is a useful distension media, it does not allow the clearing of blood and debris during the procedure. Complications may arise from gas embolism. For these

reasons, we used sterile physiological serum as the distension medium (Griffols, S.A). The system of distension used was a pressure bomb (Endomat Hamou Karl Storz).

4.5 ENDOMETRIAL STUDY

4.5.1 Wide Genomic Analysis.

4.5.1.1 Tissue Collection

Endometrial biopsies were collected with Pipelle catheters (Gynetics Medical Products N.V, #4164 probet, Belgium) under sterile conditions from the uterine fundus. One half of each sample was snap-frozen in liquid nitrogen and stored at -70°C until further processing.

4.5.1.2 RNA Isolation

Total RNA was extracted using the Trizol method according to the protocol recommended by the manufacturer (Life Technologies, Inc., Gaithersburg, MD). In short, homogenised biopsies (1 ml Trizol reagent/75 mg tissue) were incubated at room temperature for 5 min, chloroform (0.2 volumes of Trizol) was added, and the samples were incubated for 2.5 min at room temperature. Thereafter, the samples were centrifuged for 15 min at 12,000 g (4°C). The aqueous phase was precipitated with an equal volume of 2-propanol, stored in ice for 5 min and centrifuged for 30 min at 12,000 g (4°C). The pellet was washed with 75% ethanol and dissolved in DEPC-treated water. The integrity of the RNA samples (RNA quality control

procedure) was assessed using the 2100 bioanalyzer (Agilent Technologies, Madrid, Spain) by running an aliquot of the RNA samples on the RNA 6000 Nano LabChip (Agilent Technologies, Madrid, Spain). All the samples had to obtain a RNA integrity number index (RIN) greater than 7 in order to be included in the analysis.

4.5.1.3 Microarray Hybridisation Procedure

All samples were hybridised onto the Whole Human Genome Oligo Microarray (Agilent Technologies, Madrid, Spain) encompassing more than 44,000 human DNA probes. The protocols for sample preparation and hybridisation of the endometrial samples were adapted from the Agilent Technical Manual. Briefly, first-strand cDNA was transcribed from 1 mg of total RNA using T7-Oligo (dT) promotor primer. Samples were in vitro transcribed and Cy-3 labelled with the Quick-AMP labelling kit *(Agilent Technologies, Madrid, Spain*). The cRNA synthesis typically yielded between 10 and 15 µg. Following a further clean-up round *(QIAGEN, Barcelona, Spain),* cDNA was fragmented into pieces ranging from 35 to 200 bases, which were confirmed using Agilent 2100 Bioanalyzer technology. Fragmented cRNA samples (1.65 µg) were hybridised onto chips through 17 h of incubation at 65ºC with constant rotation; then, microarrays were washed in two washing buffers for 1 min each *(Agilent Technologies, Madrid, Spain).* Hybridised microarrays were scanned in an Axon 4100A scanner

(Molecular Devices, Sunnyvale, CA, USA) and data extracted with GenePix Pro 6.0 software *(Molecular Devices, Sunnyvale, CA, USA).*

4.5.1.4 Data Processing and Data Analysis

GenePix Pro 6.0 software was used for array image analysis and the calculation of spot intensity measurements, which were used as raw data. Spot intensities (medians) without background subtraction were transformed to the log2 scale. Before quantile normalisation, data were represented in a box plot to check the data distribution, and abnormal microarray data were discarded. The replicates by gene symbol were merged, and the data were filtered to delete unknown sequences or probes without a gene description.

The R statistical software system was used for these purposes and for downstream analysis [91].

The gene expression profile was determined by comparing the experimental groups with the control group (2 by 2 comparisons) with non-parametric tests. Two criteria were used to define genes that had altered mRNA abundance between the different sample sets: an absolute fold change of 2.0 or more and a corresponding fold change p-value lower than 0.05.

4.5.1.5 Functional Analysis

To detect activations or inactivations of biological functions or pathways, we used the Database for Annotation, Visualization and Integrated Discovery (DAVID) [92], a gene set-based algorithm that detects significantly

represented functionally related genes in lists of genes ordered by differential expression. DAVID can search blocks of functionally related genes by different criteria, such as gene ontology terms or KEGG pathways.

Search Tool for the Retrieval of Interacting Genes/Proteins (STRING) [93] represents the connexions among the differentially expressed genes. This bioinformatics tool provides information about a comprehensive and regulated group of protein associations for a large number of organisms.

4.5.1.6 Clustering and Principal Components Analysis

Expression data were normalised by Z-score. Hierarchical clustering was performed with MeV 4.2.02 software (http://www.tm4.org) [94] with a complete-linkage hierarchical clustering algorithm and visualised by the same software. Euclidean distance was chosen as the similarity measure.

Principal components analysis (PCA) was performed using the MeV 4.2.02 software. The data table of rows (genes) and columns (endometrial samples) was transposed and PCA was run to reduce the number of variables to two or three principal components representing the majority of the variability in the dataset. A two- or three-dimensional scatter plot was produced to visualise the differences between the sample sets (Control, 18 h, 3 d and 5 d) based on each sample's gene expression profile.

4.5.2 Immunohistochemical Study

Immunohistochemical analysis of PRA and PRB.

The method used for determining the progesterone receptor was the avidin-biotin immunohistochemistry method (ABC system, Dako Ltd., Cambridge, UK) with 3, 3´-diaminobenzidine as the chromagen. Secondary antibodies are conjugated to biotin and function as links between tissue-bound primary antibodies and an avidin-biotin-peroxidase complex (Fig. 7).

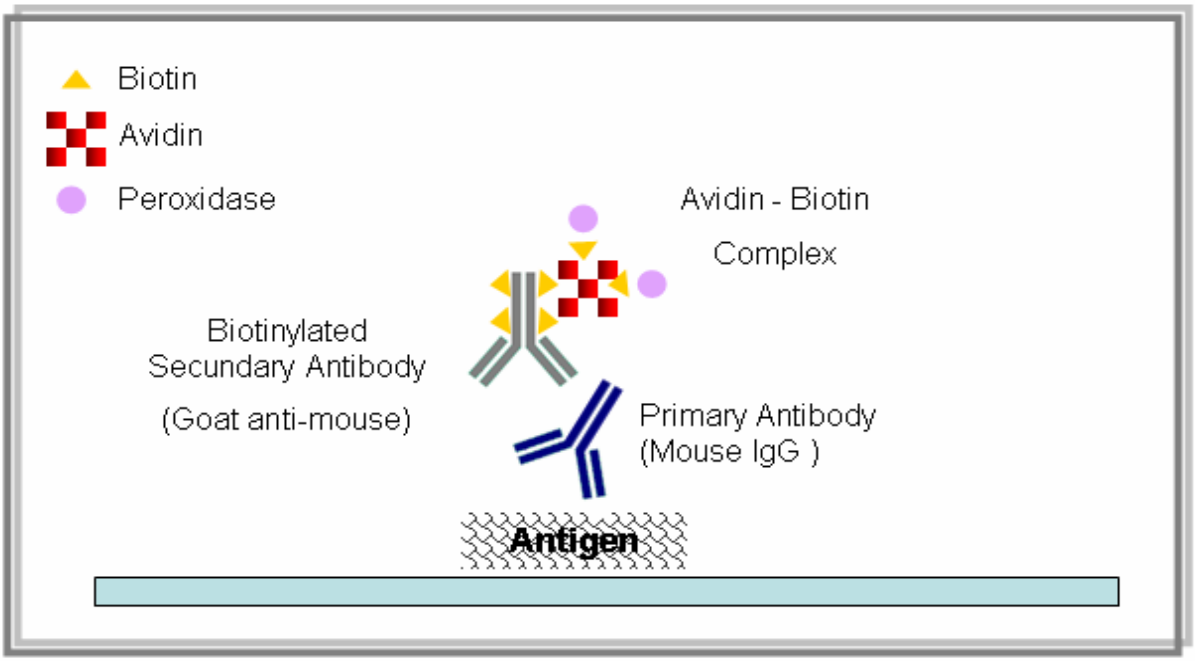

Figure 7: Avidin-Biotin Complex Method

Whereas polyclonal antibodies are multiple antibodies produced by different types of immune cells that recognise the same antigen, monoclonal antibodies are derived from a single cell line (also referred to as a clone). The antibody chosen to detect the progesterone receptor in this experiment was a

monoclonal antibody.

Solutions:

-Sodium citrate autoclaved in the pressure cooker (PC): 1.8 L of deionised/distilled water + 200 ml of sodium citrate (0, 1 M, pH: 6.0).

-Solution of hydrogen peroxide in distilled water. Peroxide (30% w/w SIGMA H1009). Final solution: 3%.

-PBS: 1X concentration (P5368, SIGMA).

-Serum block NGS/PBS/BSA mix (1 ml NGS/4 ml PBS/ 5% BSA): 1 ml of NGS + 4 ml of PBS + 5% BSA. As we prepared 5 ml, we weighed 0.5 g of BSA powder and mixed with 2.000 µl NGS and 8.000 µl of PBS for a final volume of 10 ml. NGS (Vector Laboratories, BIOSERA S1000, PBS (P5368, SIGMA) and BSA (A9647 SIGMA).

-Vector Laboratories biotin/avidin blocking kit (Avidin blocking kit Vector Laboratories SP2061).

-Primary Antibody: Mouse IgG monoclonal (Novocastra NCL-PGR A/B forms). We tested two dilutions (1:40 and 1:100), but we only obtained valid data for one of them (dilution 1:100). Concentration: 45 mg/l in serum block.

-Negative control: Mouse IgG (SIGMA) at the same concentration:

First: 9 µl of Mouse IgG sigma in 191 µl of block: This is the negative dilution. Second: 5 µl of the negative dilution in 195 µl of block: this is the

negative final.

-For the positive control, we used samples from the mid-secretory phase and proliferative phase at a dilution of 1:40.

-Secondary antibody: We prepared 1 ml of 1:200 dilution of biotinylated goat anti-mouse (Vector Labs BA9200), 1.600 µl of block + 8 µl of antibody.

-PBST: 400 ml of PBS (PBS1 SIGMA)+ 200 µl of Tween (P9416 SIGMA)+ 3.2 g of NaCl (S3014 SIGMA).

-Tertiary antibody: RTU (ABC Elite Reagent), 3 drops each slide, for 30 minutes at room temperature.

-DAB (3, 3'-diaminobenzidinetrahydrochloride) (Vector Laboratories ImmPACT™ DAB Peroxidase substrate SK-4105): 2 drops into 2.000 µl of diluent and we put it into aluminium boil.

-Mayer's haematoxylin solution (Vector Laboratories).

Procedure:

Tissue fixation was accomplished with formalin (4%) (7040 JT Bake). The tissue fixation medium was replaced by wax, washed through a series of solutions with ethanol concentrations increasing to 100%(100986.1000, Merck, Spain), followed by xylene (Panreac Quimica S.A.U) and then hot wax (253211.1211, Panreac Quimica S.A.U). This process stabilises the tissue

(wax) to make cutting the sections easier. The tissue sections were cut at five microns and enclosed in cassettes (631-9614, VWR International Eurolab, S.L. Spain).

Five-micrometre paraffin-embedded sections were dewaxed in xylene (Panreac Quimica S.A.U) twice for 5 minutes each and rehydrated in sequential solutions of ethanol absolute, 95º and 70º (818760 EMPLURA®, Merck, Spain), for 20 seconds in each. After that, slides were rinsed and kept in tap water.

Antigen retrieval was performed by autoclaving sections for 5 minutes in boiling 0, 02 M sodium citrate (pH 6.0), and allowing 20 minutes to cool down. Afterwards, the slides were rinsed and kept in tap water.

It is necessary to block the endogenous peroxidase activity with 3% (vol/vol) hydrogen peroxide in distilled water for 30 seconds at room temperature. Afterwards, we washed the slides twice with PBS, and then they were put in the Sequenza cover plates (Thermo-Shandon, 72110013). The rest of steps were performed with the slides in the Sequenza system.

A Vector Laboratories biotin/avidin blocking kit was used for 15 minutes at room temperature to block biotin and avidin binding sites. We added three drops to each slide. Then, we washed the slides twice in PBS and included 125 µl of serum block NGS/PBS/BSA mix on every slide.

Sections were incubated with the primary antibody (NCL-Progesterone)

or with mouse IgG (negative control) overnight at 4°C. Slides were washed 2 times in PBST.

Subsequently, they were incubated with biotinylated secondary antibodies. We put 125 µl of the dilution of goat anti-mouse antibody on each slide and waited for 30 minutes.

Sections were again washed twice in PBST and incubated with the tertiary antibody RTU (ABC Elite Reagent). After that, we washed them in PBS and removed the excess Sequenza from the solution.

The site of bound enzymes was identified by application of 3, 3-diaminobenzidine in H2O2 to the samples for 5 minutes. Subsequently, they were washed with tap water for 5 minutes.

We counterstained with nuclear solution of haematoxylin for 20 minutes. Later, we washed the sections with tap water for 30 minutes and dehydrated them for 20 seconds with consecutive alcohols (70%, 80%, and 95%) and absolute alcohol and for 5 seconds with xylene. To finish the fixation, a drop of Pertex on a cover slip was placed on the sample.

Immunohistochemical analysis of prokineticin 1 (PROK-1) and the prokineticin 1 receptor (PROK-R1).

We used a similar method for this analysis: the labelled streptavidin-biotin (LSAB) method (Dako Ltd., Cambridge, UK). This method also utilises a biotinylated secondary antibody that links primary antibodies to a conjugated streptavidin peroxidase. In this case, the antibody chosen to detect the PROK-1 and PROK-R1 expression was a polyclonal antibody (Fig. 8).

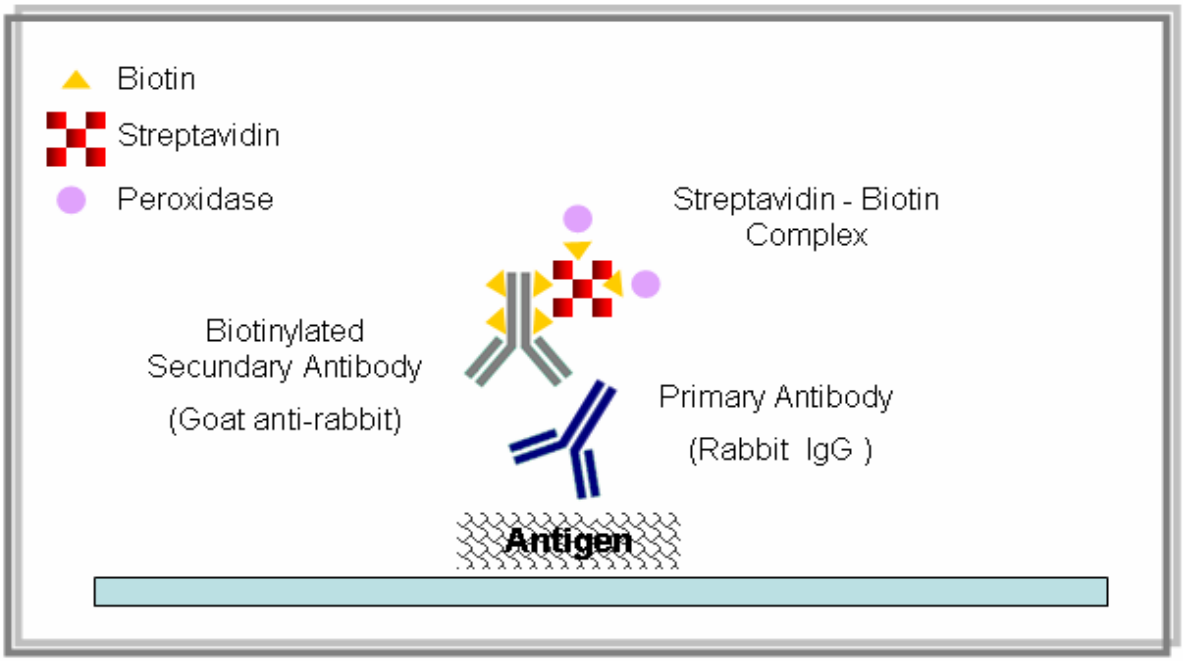

Figure 8: Labelled Streptavidin-Biotin (LSAB) Method.

Solutions:

-Sodium citrate autoclaved in the pressure cooker (PC): 1.8 L of deionised/distilled water + 200 ml of sodium citrate (0, 1 M, pH: 6.0).

-Solution of 90 ml of methanol + 10 ml hydrogen peroxide.

-TBS: 1.800 ml of water + 200 ml of TBS (10x) (stored at 4ºC), (T6664, SIGMA).

-Serum block NGS/TBS/BSA mix (1 ml NGS/4 ml TBS/ 5% BSA): 1 ml of NGS + 4 ml of PBS + 5% BSA. We prepared 5 ml; we weighed 0.25 g of BSA powder and mixed with 1.000 µl NGS and 4.000 µl of TBS for a final volume of 5 ml. NGS (Vector Laboratories, BIOSERA S1000), TBS (T6664, SIGMA) and BSA (A9647 SIGMA).

-Vector laboratories biotin/avidin blocking kit (Avidin blocking kit Vector Laboratories SP2061).

-Primary antibody PROK-1: Rabbit polyclonal PROK-1 (Phoenix Pharmaceuticals H-023-59 Inc., Belmont, CA) at a dilution of 1:1000 in NGS/TBS/BSA mix.

-Primary antibody PROK-1R-1: Rabbit polyclonal PROK-1R-1 (MBL; LS-A6684) (1:250).

-Negative control: Rabbit IgG (Dako X0903) at an equivalent concentration to the antibody used (it was prepared with normal-goat serum (NGS) mix at a dilution of 1:1000 for PK1 and 1:250 for PKR1).

-For the positive control, we used samples from the mid-secretory phase and proliferative phase at a dilution of 1:250.

-Secondary antibody (PROK-1 and PROK-R1): Biotinylated goat anti-rabbit (Vector Labs BA 6000). We prepared 1 ml at 1:200 dilution (1000 µl of block + 5 µl of antibody).

-Tertiary antibody (PROK-1 and PROK-R1): HRP conjugated streptavidin 1:1000 in TBS (K5001 Dako REAL™ Detection Systems (LSAB+)).

-DAB (3, 3'-diaminobenzidinetrahydrochloride) (Vector Laboratories ImmPACT™ DAB Peroxidase substrate SK-4105): 2 drops into 2.000 µl of diluent and we put it into aluminium boil.

-Mayer's haematoxylin solution (Vector Laboratories).

Procedure:

Tissue fixation was accomplished with formalin (4%) (7040 JT Bake). The tissue fixation medium was replaced by wax and washed with ethanol solutions at a series of concentrations increasing to 100% (100986.1000, Merck, Spain), followed by xylene (Panreac Quimica S.A.U) and hot wax (253211.1211, Panreac Quimica S.A.U). This process stabilises the tissue (wax) to make cutting the sections easier. The tissue sections were cut at five microns and enclosed in cassettes (631-9614, VWR International Eurolab, S.L. Spain).

Five-micrometre paraffin-embedded sections were dewaxed in xylene (Panreac Quimica S.A.U) twice for 5 minutes each and rehydrated in

sequential solutions of ethanol absolute, 95º and 70º (818760 EMPLURA®, Merck, Spain) for 20 seconds in each solution. Subsequently, the slides were rinsed and kept in tap water.

Antigen retrieval was performed by autoclaving sections for 5 minutes in boiling 0, 02 M sodium citrate (pH 6.0) and then allowing 20 minutes for cool down. Later, the slides were again rinsed with tap water.

We blocked the endogenous peroxidase activity with 3% (vol/vol) hydrogen peroxide in methanol for 30 seconds at room temperature.

From this point, all washes were performed in a humidity chamber. First, we washed slides twice for 5 minutes each in TBS.

As in the previous protocol, Vector Laboratories biotin/avidin blocking kit was used for 15 minutes at room temperature to block biotin and avidin binding sites. Then, we washed the slides twice in TBS.

We added 50 µl of serum block NGS/TBS/BSA mix to every slide for 30 minutes at room temperature.

Sections were incubated with the primary antibody, rabbit antihuman polyclonal PROK-1 antibody (1:1000 in NGS mix) or rabbit polyclonal PROK-1R-1 antibody (1:250 in NGS mix) overnight with a glass at 4º C. The slides were then washed twice for 5 minutes in TBS.

Two negative controls were used at the same concentration of primary

antibody:

-No primary antibody addition.

-Rabbit IgG at an equivalent concentration to the antibody used (prepared with normal-goat serum (NGS) mix at a dilution of 1:1000 for PK1 and 1:250 for PKR1. We added 100 µl of the dilution of goat anti-rabbit antibody to each slide and waited for 30 minutes. Afterwards, we washed the slides in TBS twice for 5 minutes each.

Samples were incubated with the tertiary antibody-HRP conjugated streptavidin in TBS at a dilution of 1:1000 for 30 minutes at room temperature and then washed again in TBS twice for 5 minutes each.

The sections were placed in DAB solution for 5 minutes and then washed with tap water for 5 minutes. To counterstain, we used a nuclear solution of haematoxylin for 20 minutes. Subsequently, we washed the sections with tap water for 30 minutes.

We dehydrated the samples for 20 seconds with consecutive alcohols (70%, 80% and 95 %) and absolute alcohol and for 5 seconds with xylene. To finish the fixation, a drop of Pertex on a cover slip was placed on the sample.

Immunohistochemical analysis of leukaemia inhibitory factor (LIF)

The same method (avidin-biotin immunohistochemistry method ABC) as in the first immunohistochemical experiment (PR) was used. The antibody was a polyclonal subtype. The specific solutions and the steps taken in the process follow:

Solutions:

-Sodium citrate autoclaved in the pressure cooker (PC): 1.8 L of deionised/distilled water + 200 ml of sodium citrate (0, 1 M, pH: 6.0).

-Solution of hydrogen peroxide in distilled water. Peroxide (30% w/w SIGMA H1009). Final solution: 3%.

-PBS: 1X concentration (P5368, SIGMA).

-Serum blocker NHS/PBS/BSA mix (1 ml NGS/4 ml PBS/5% BSA): 1 ml of NHS + 4 ml of PBS + 5% BSA. To prepare 5 ml, we weighed 0.5 g of BSA powder and mixed with 2.000 µl NHS and 8.000 µl of PBS for a final volume of 10 ml. NHS (Vector Laboratories, BIOSERA S2000), PBS (P5368, SIGMA) and BSA (A9647 SIGMA).

-Vector laboratories biotin/avidin blocking kit (Avidin blocking kit Vector Laboratories SP2061).

-Serum blocker: NHS (normal horse serum)/BSA/PBS at the same

concentration.

-Primary antibody LIF: Goat polyclonal LIF antibody (AB-250-NAR&D Systems). We tested two concentrations: 1:50 and 1:25 in NHS/PBS/BSA mix. Negative control was goat IgG (R&D Systems, AB-108-C) at equivalent concentration.

-For the positive control, we used samples from the mid-secretory phase and proliferative phase at dilutions of 1:50 and 1:25.

-Secondary antibody: Biotinylated rabbit anti-goat (Vector Labs BA5000) at a dilution of 1:200.

-Tertiary antibody: RTU (ABC Elite Reagent).

-DAB (3, 3'-diaminobenzidinetrahydrochloride) (Vector Laboratories ImmPACT™ DAB Peroxidase substrate SK-4105): 2 drops into 2.000 µl of diluent and we put it into aluminium boil.

-Mayer's haematoxylin solution (Vector Laboratories).

Procedure:

Tissue fixation was accomplished with formalin (4%) (7040 JT Bake). The tissue fixation medium was replaced by wax, washed with a series of ethanol solutions at concentrations increasing to 100% (100986.1000, Merck, Spain), followed by xylene (Panreac Quimica S.A.U) and then hot wax (253211.1211, Panreac Quimica S.A.U). This process stabilises the tissue

(wax) to make cutting the sections easier. The tissue sections were cut at five microns and enclosed in cassettes (631-9614, VWR International Eurolab, S.L. Spain).

Five-micrometre paraffin-embedded sections were dewaxed in xylene (Panreac Quimica S.A.U) twice for 5 minutes each and rehydrated in sequential solutions of ethanol absolute, 95º and 70º (818760 EMPLURA®, Merck, Spain) for 20 seconds in each solution. Then, the samples were rinsed and kept in tap water.

Antigen retrieval was performed by autoclaving sections for 5 minutes in boiling 0, 02 M sodium citrate (pH 6.0), and allowing 20 minutes to cool down. Then, the slides were again rinsed and kept in tap water. To block the endogenous peroxidase activity, we incubated slides with 3% (vol/vol) hydrogen peroxide in distilled water for 10 minutes at room temperature. From this point, all washes were performed in a humidity chamber. The first step was to wash the slides in PBS twice for 5 minutes each. Next, we blocked biotin and avidin binding sites with a Vector Laboratories biotin/avidin blocking kit for 15 minutes at room temperature. Then, we washed the slides twice in PBS. We added 50 µl of serum block NHS/TBS/BSA mix to every slide for 30 minutes at room temperature. Sections were incubated with the primary antibody, goat anti-human polyclonal LIF antibody (1:50 and 1:25 in NHS mix), and overnight at 4 ° C. They were washed in TBS 2 times for 5 minutes. The negative control was goat IgG at an equivalent concentration of primary antibody. Then, we

washed slides twice for 5 minutes each in PBS. Subsequently, samples were incubated with biotinylated secondary rabbit anti-goat antibodies at a dilution of 1:200 and then allowed to rest for 30 minutes. Sections were again washed twice in PBS and incubated with the tertiary antibody RTU (ABC Elite Reagent).

DAB solution was applied as the chromagen for 5 minutes; then, the slides were washed for 5 minutes with tap water. We counterstained with nuclear solution of haematoxylin for 20 minutes. Next, we washed the sections with tap water for 30 minutes. To dehydrate the samples, we incubated them for 20 seconds with consecutive alcohols (70%, 80%, and 95%) and absolute alcohol and for 5 seconds with xylene. Finally, to complete the fixation, a drop of Pertex on a cover slip was placed on each sample.

5. RESULTS

5.1 SAFETY AND STABILITY STUDY.

The patients were asked to report any feelings of discomfort after insertion of the device. In addition, each patient was extensively monitored. In all cases, the device was introduced under ultrasound monitoring without any complications. It was subsequently removed after 24 hours in five of the patients (group 1) and after 6 days in the other 3 (group 2).

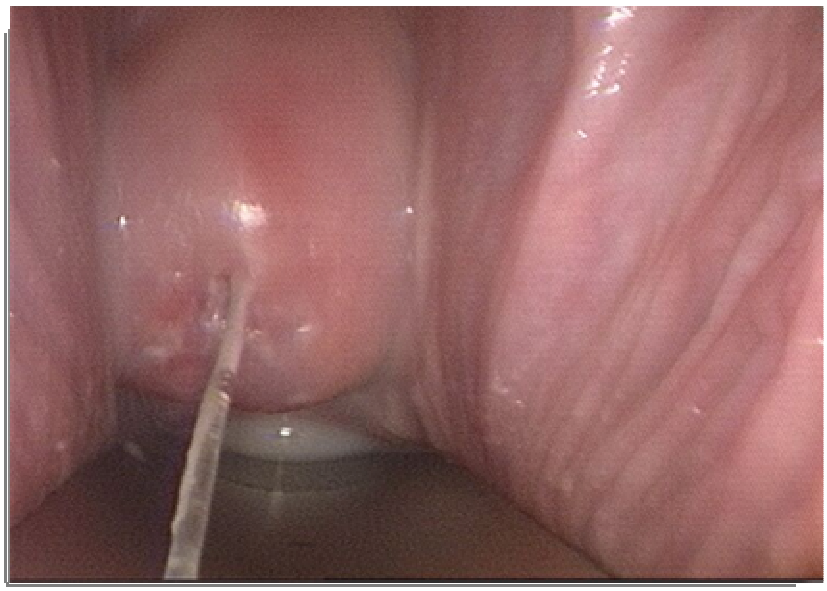

Figure 9: Anecova device retrieval after 6 days inside the endometrial cavity.

Three of nine patients (3/9) had the device displaced to the isthmus, and it was observed in the internal os. When the device was removed, we did not observe any alteration in the uterine cavity. In one case the device was expelled on the day of insertion. Only one of the patients suffered symptoms such as sweating and dizziness, but this woman was reported to be prone to having fainting fits and low blood pressure. Another patient reported

pain in the left ovary that was not associated with the presence of the device.

During the hysteroscopic examination, we noticed an isthmical stenosis in one patient close to the area of the caesarean section with a normal cavity. This patient showed a small inflammatory reaction in the vessels located in the left posterior side of the endometrial cavity that was probably due to the insertion of the device.

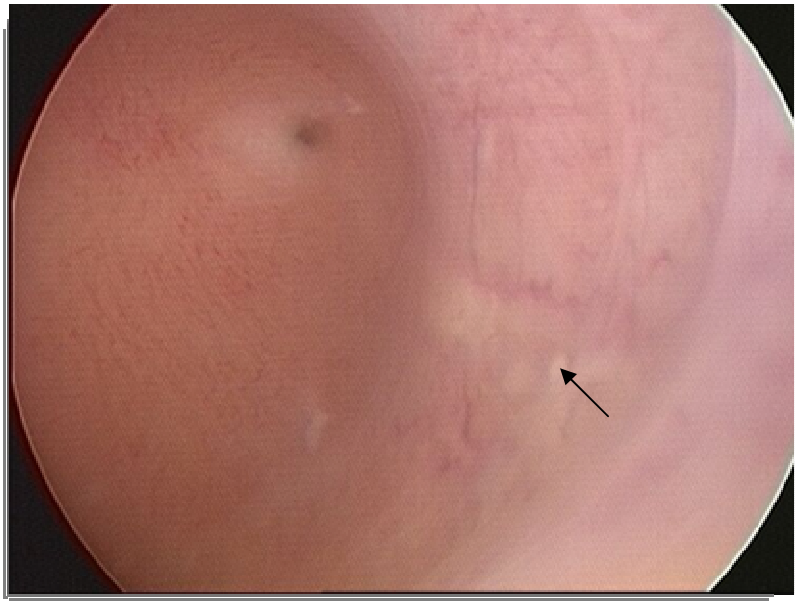

Figure 10: Picture of endometrial cavity taken during hysteroscopy. A slight Anecova device fingerprint is observed in the left endometrial side pointing towards the tubal ostium (arrow).

In another patient, we observed focal hyperaemia during the extraction process. Three days earlier, this patient had suffered abdominal pain and abdominal distension.

Figure 11: Picture of endometrial cavity taken during hysteroscopy. Slight hyperaemia extended over the endometrium.

None of the patients felt serious pain, sickness, bleeding or subjective perception of feeling the device. In addition, all patients reported normal menstruation in the next cycle after removal of the device.

5.2 *Wide Genomic Analysis*.

5.2.1 RNA Quality

RNA integrity was based on a procedure that involves the separation of RNA into differently sized fragments by capillary electrophoresis molecular sieving, with results shown on an electropherogram. The program calculates an RNA integrity number (RIN) index. All samples obtained a RIN greater than 7.5, except sample ANE-11 with a RIN of 6.7, which was excluded from the analysis (Table 1).

Code	[RNA] (ng/µL)	RIN	Group
ANE-1	2770	8.9	Control
ANE-4	1125	8.7	Control
ANE-7	2110	8.9	Control
ANE-9	1065	7.5	18h
ANE-10	950	8.3	3d
ANE-11	1360	6.7	5d
ANE-12	2040	9.0	5d
ANE-13	2270	8.4	18h
ANE-14	1500	8.4	18h
ANE-15	1870	8.5	5d
ANE-16	875	7.7	5d
ANE-17	1965	9.0	3d
ANE-18	1000	8.5	Control
ANE-19	955	8.1	Control
ANE-20	830	8.0	3d
ANE-22	1505	8.1	3d
ANE-23	1925	8.8	3d
ANE-24	970	9.3	18h
ANE-25	2190	8.8	18h
ANE-26	2550	9.3	5d

Table 1: The RIN data correspond to the RNA integrity. Sample ANE-11, with a RIN of 6.7, was excluded from the analysis.

5.2.2 Identification of Altered Gene Expression

In the log2 transformation, we detected outliers in the low-RIN sample and two more samples (ANE-9, ANE-10). These two samples were also excluded (Fig. 12). In statistics, an outlier is an observation that is numerically distant from the rest of the data.

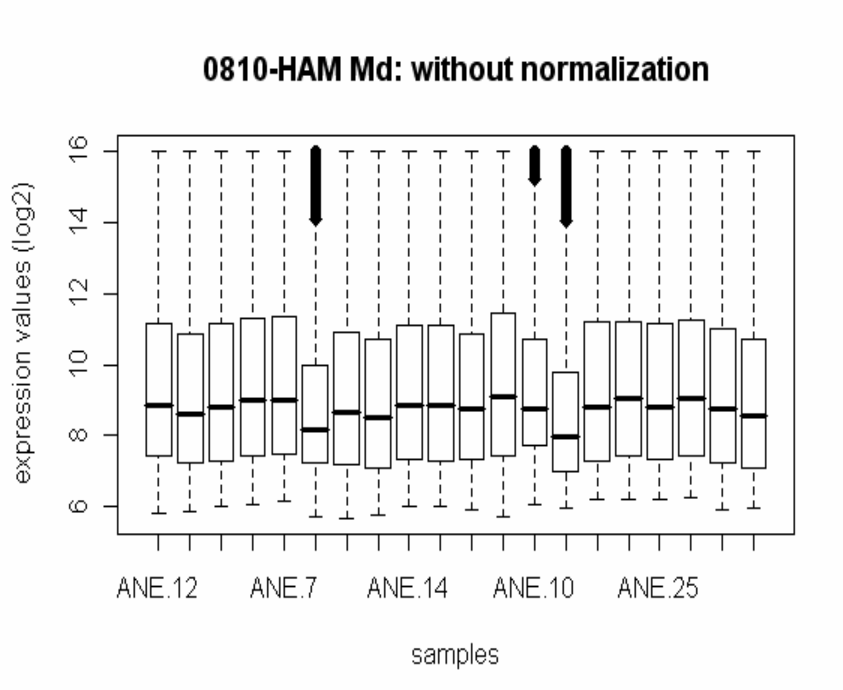

Figure 12: Box-plot representation of the log2-transformed median for all samples; black arrows indicate outliers.

The final number of samples in the analysis was 17. We show the normalised data in Figure 13.

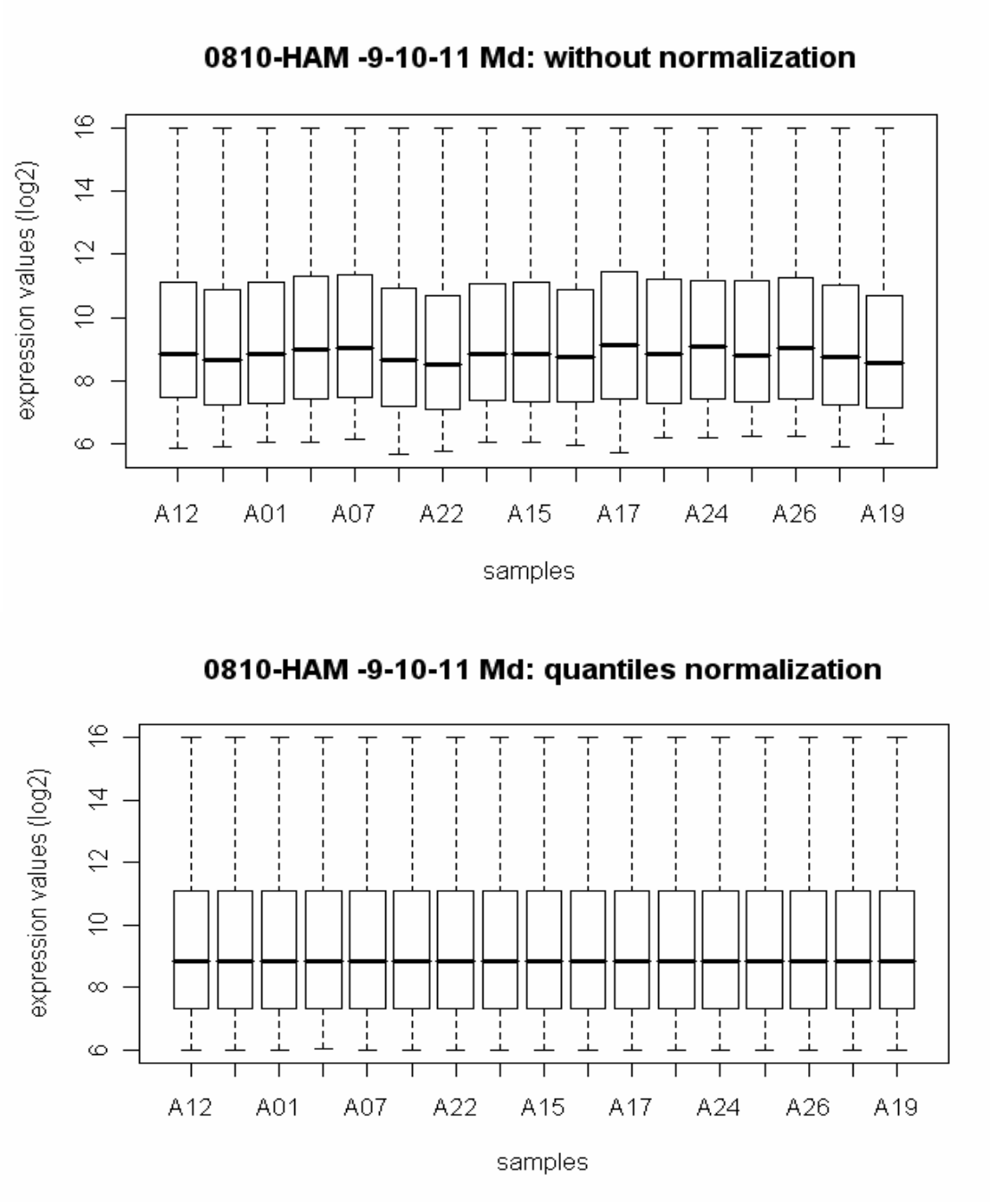

Figure 13. Box-plot representation of the log2-transformed medians for 17 samples (excluding ANE-9, ANE-10 and ANE-11). Even without normalising the box-plots are quite similar. Box-plot representation of the normalised data.

To evaluate the effect of the Anecova device on the gene expression pattern of the endometrium, the data were analysed by comparing each experimental group (18 h, 3 d or 5 d) with the control group (Table 2, annex). The number of dysregulated genes in each group is indicated in Table 3.

Non-parametric tests

Comparison	UP	Down
18h vs Control	10	6
3d vs Control	57	78
5d vs Control	11	9
18h-3d-5d vs Control	7	3

Table 3: Comparison of samples (n=5) exposed to the device for 18 hours, 3 days or 5 days against the control samples (women who were not exposed to the device, whose biopsy was taken on day 5 after follicular punction). This table only summarises the number of probes with an upward or downward fold change greater than 2 and statistical significance lower than 0.05.

In the comparison between endometrial gene expression with device insertion for any period of time (18 h, 3 d and 5 d) versus control samples, the number of dysregulated DNA probes was 10 (7 up- and 3 down-regulated), but not all of them were known genes (Table 4).

UP	pvalue	FC	Symbol	Description
NM_139172	0,0000	**4,44**	MDAC1	Homo sapiens MDAC1 (MDAC1), mRNA [NM_139172]
AK097517	0,0000	**3,01**	LOC283767	Homo sapiens cDNA FLJ40198 fis, clone TESTI2019975, weakly similar to TRICHOHYALIN. [AK097517]
NM_005252	0,0000	**2,52**	FOS	Homo sapiens v-fos FBJ murine osteosarcoma viral oncogene homolog (FOS), mRNA [NM_005252]
NM_021114	0,0000	**2,18**	SPINK2	Homo sapiens serine peptidase inhibitor, Kazal type 2 (acrosin-trypsin inhibitor) (SPINK2), mRNA [NM_021114]
XM_498537	0,0000	**2,09**	LOC440084	PREDICTED: Homo sapiens hypothetical LOC440084 (LOC440084), mRNA [XM_498537]
NM_000558	0,0000	**2,08**	HBA1	Homo sapiens hemoglobin, alpha 1 (HBA1), mRNA [NM_000558]
AK055838	0,0000	**2,07**	AK055838	Homo sapiens cDNA FLJ31276 fis, clone KIDNE2006376, weakly similar to GAMMA-GLUTAMYLTRANSPEPTIDASE 1 PRECURSOR (EC 2.3.2.2). [AK055838]
DOWN	**pvalue**	**FC**	**Symbol**	**Description**
NM_006952	0,0000	**-2,49**	UPK1B	Homo sapiens uroplakin 1B (UPK1B), mRNA [NM_006952]
AK096051	0,0000	**-2,48**	LOC348174	Homo sapiens cDNA FLJ38732 fis, clone KIDNE2010750. [AK096051]
AK126241	0,0175	**-2,06**	FLJ44253	Homo sapiens cDNA FLJ44253 fis, clone TKIDN2009092. [AK126241]

Table 4: Comparison between the samples exposed to the device vs. controls. Summary of the number of probes with a fold-change larger than 2 or smaller than -2 and a statistical significance lower than 0.05 in all mentioned comparisons. The genes are named according to the database of the National Center for Biotechnology Information (NCBI).

Only two genes were dysregulated in all study groups. Four genes coincided between the 3-day and 5-day groups. Finally, four different genes were identified that coincided between the 18-hour and 3-day groups (Fig. 14).

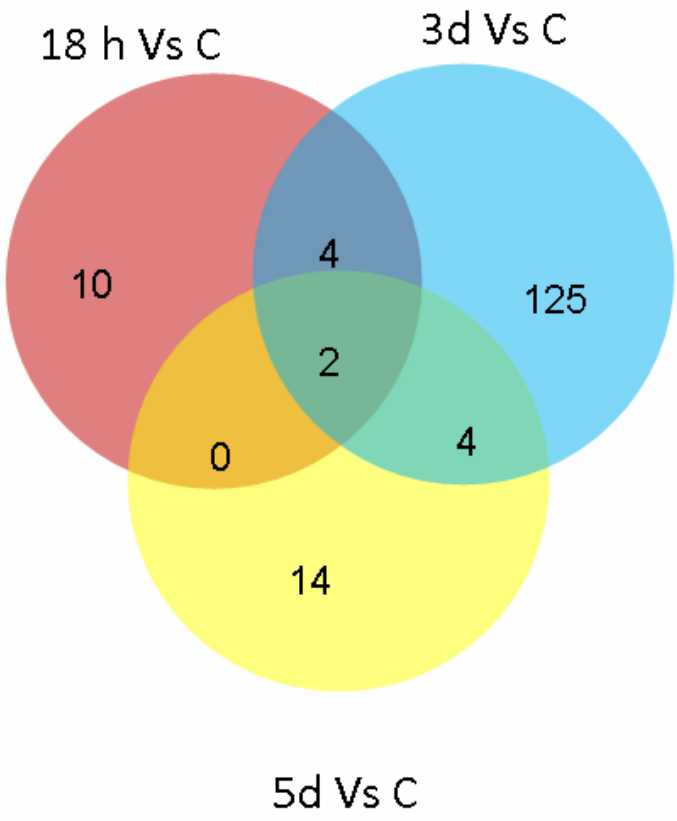

Figure 14: This diagram shows the number of dysregulated genes that coincided in the three groups (device inside uterus for 18 hours, 3 days or 5 days vs. control samples).

When the sequences were analysed to determine the relations among them (STRING), there was no statistical relationship with any gene ontology term. The DAVID Database was also used to study the expression of these sequences. We learned that only the endometrium samples from the 3-day group showed more differences than the control samples did.

Thirty-three of the dysregulated genes with a p-value lower than 0.05 were related to multicellular organismal processes; 4 had a relationship with metabolic processes (oxygen and reactive oxygen species); 17 had transporter activity; and 3 were related to gamma-glutamyltransferase activity and 5

were related to arachidonic-acid metabolism. We also noticed that four dysregulated genes in the 3-day insertion group had a direct relationship with glutathione metabolism.

5.2.3 Clustering

An unsupervised hierarchical clustering was performed for the 17 endometrial biopsies. This analysis revealed that endometrial samples from subjects with the Anecova device, regardless of their duration of exposure, and from controls, clustered irrespective of their origin, do not show differences in the global gene expression profiles (Fig. 15).

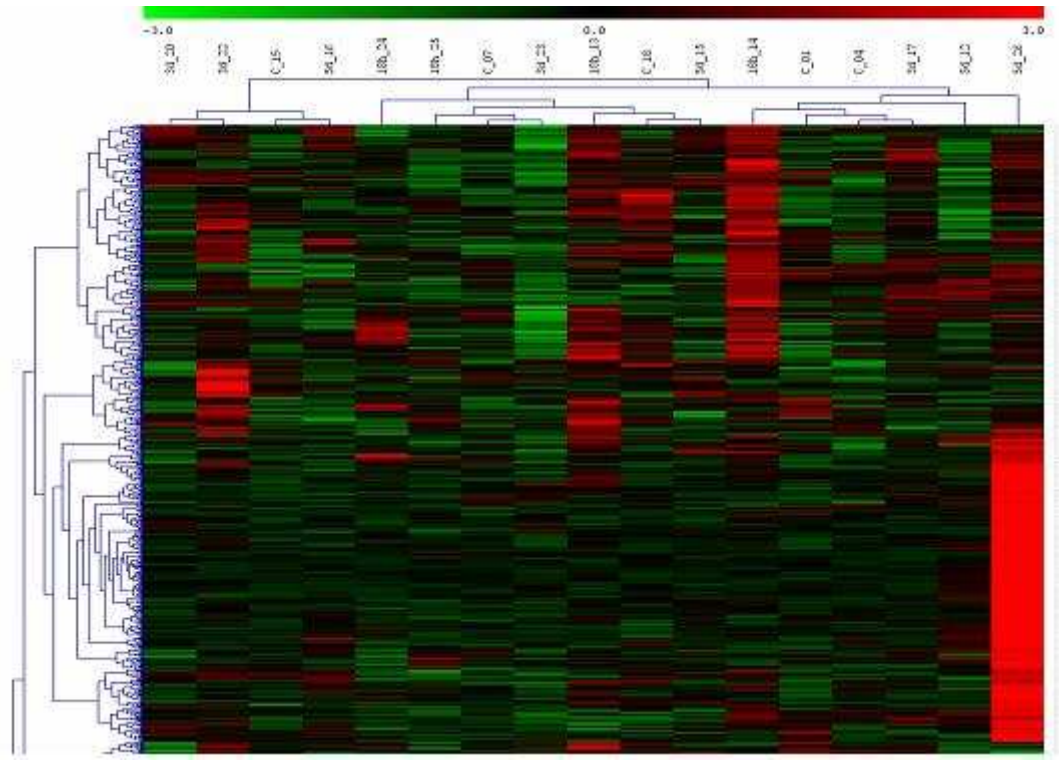

Figure 15: Cluster analysis revealed no differences in the global gene expression profiles among specimens.

5.2.4 PCA (Principal Components Analysis)

When PCA was applied to data, samples with similar trends in their gene expression profiles tended to cluster close together in the plot. In this case, the samples from each group do not have similar trends in their expression profiles and do not cluster close together, suggesting no genomic impact of the device on the endometrium (Fig. 16).

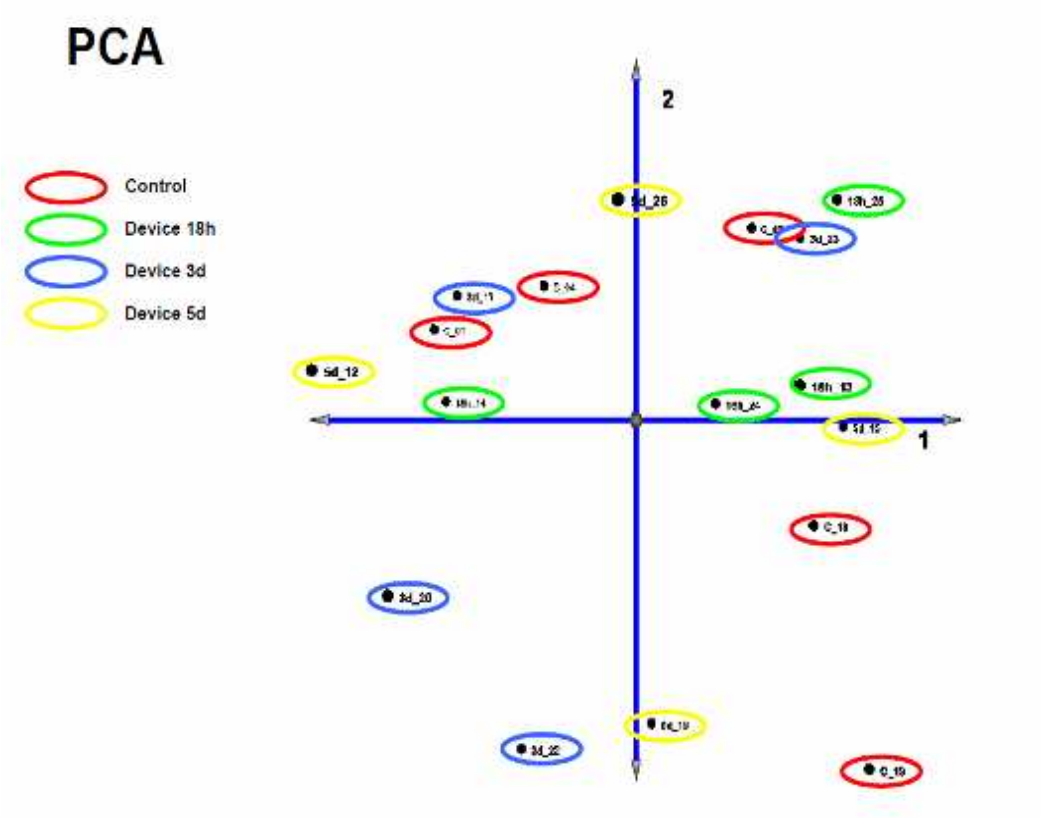

Figure 16: PCA demonstrates the variability among groups, suggesting no identifiable endometrial effect.

5.3 IMMUNOHISTOCHEMISTRY STUDY

5.3.1 Scoring System and Summary Slides Data

The immunostaining intensity of all tissue sections was scored on a four-point scale, where (-) = no staining, (+/-) = slightly positive, (+) = weakly positive, and (++) = strongly positive. The score depended on the intensity of staining expressed by most of the cells in each chosen area. In each area (at a scale of 100X or 50X magnification), the percentage of stained cells at each scale was approximated by eye and by the same observer (Manuel Fernández-Sánchez) to avoid interobserver variability.

Immunohistochemical Localisation of Progesterone Receptors (PRA+PRB)

As expected, in the endometrial samples analysed from the three patients at day LH+7, we observed a weak staining in some nuclei of stromal cells and a very weak stain in glands. Staining was practically negative before, during and after IUD insertion (Fig. 17). The data generated are summarised in Table 5.

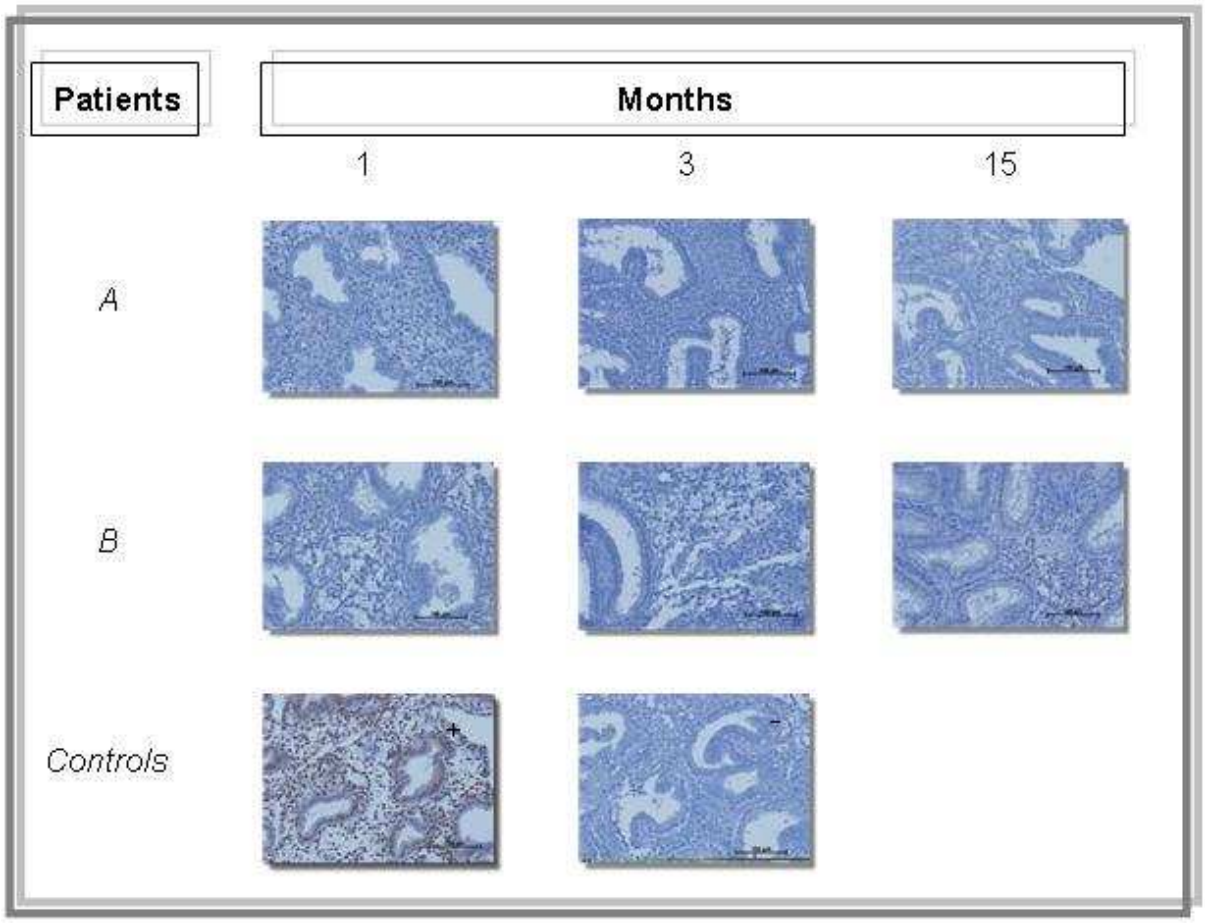

Figure 17: Immunohistochemical analysis of paraffin-embedded sections from patients A and B. Temporal expression and localisation of progesterone receptors (PRA and PRB) was detected at the mid-secretory phase. Endometrial biopsies were obtained before, during and after IUD placement, respectively, at months 1, 3 and 15. The positive control (endometrial sample at the mid-secretory phase) presents strong labelling, whereas no staining was detected in the negative control (Mouse IgG) (D). For antibody dilutions, see the Materials and Methods section.

PATIENTS	SLIDES	Glands	Stroma	Vessels/endotelium	Epithelial Surface	Nucl(N)/cyto Gland (G)/Stro (S)	Secreted
A	A,1	+/-	+/-	-	-	SN	-
	A,2	-	-	-	-	-	-
	A,3a	-	-	-	-	-	-
	A,3b	-	-	-	-	-	-
B	B,1	+/-	+/-	-	-	SN	-
	B,2	+/-	+/-	-	-	-	-
	B,3	+/-	+/-	-	-	-	-
C	C,1	-	-	-	-	-	-
	C,2	0	0	0	0	0	0
	C,3	-	-	-	-	-	-
Positive controls	MS	+	++	++	+	GN SN	-
	P	++	++	-	+	GCN SN	-
Negative control	Mouse IgG	-	-	-	-	-	-

Table 5: Designations of – (negative), +/- (weakly positive), ++ (strongly positive) and 0 (invaluable result) indicate the relative intensities of the signals. Patients are designated as samples A, B and C. P (proliferative phase) and MS (mid-secretory phase) are positive controls. Mouse IgG is the negative control.

Our results indicate that immunoreactive PRs were already down-regulated at LH+7, and this status was not modified in the presence or absence of the IUD.

Significant differences were not found in patient C's samples. In addition, comparison of these results was not possible because no valid results were obtained for patient C at month 3 (figure not shown).

Immunohistochemical localisation of PROK-1 and PROK-R1

Prokineticin 1 (PROK-1)

Immunohistochemical staining for PROK-1 was detected in the cytoplasm of glands, nuclei and cytoplasm of stromal cells, with heterogeneity among patients. As can be observed in Figure 18, a

slight decrease in stroma and glandular staining intensity was observed in the functional layer after exposure to the device compared with the pre-IUD samples in patient A. No staining was detected in vessels in the samples after IUD exposure, and few differences were found in the epithelial surface.

The intensity of immunostaining in patient B was globally very similar in the 3 biopsies, (before, during and after IUD placement); except for stronger staining in the pre-IUD epithelial surface (Fig. 18).

In patient C, there were no differences in the immunostaining (figure not shown), although we could not obtain valid results for samples at month 3.

Positive controls were all completely positive in samples at both the mid-secretory and proliferative phases. A slight expression of PROK-1 in the negative control was detected by using rabbit IgG (Fig. 18). However, there was a clear reduction in staining of this control compared with the experimental samples.

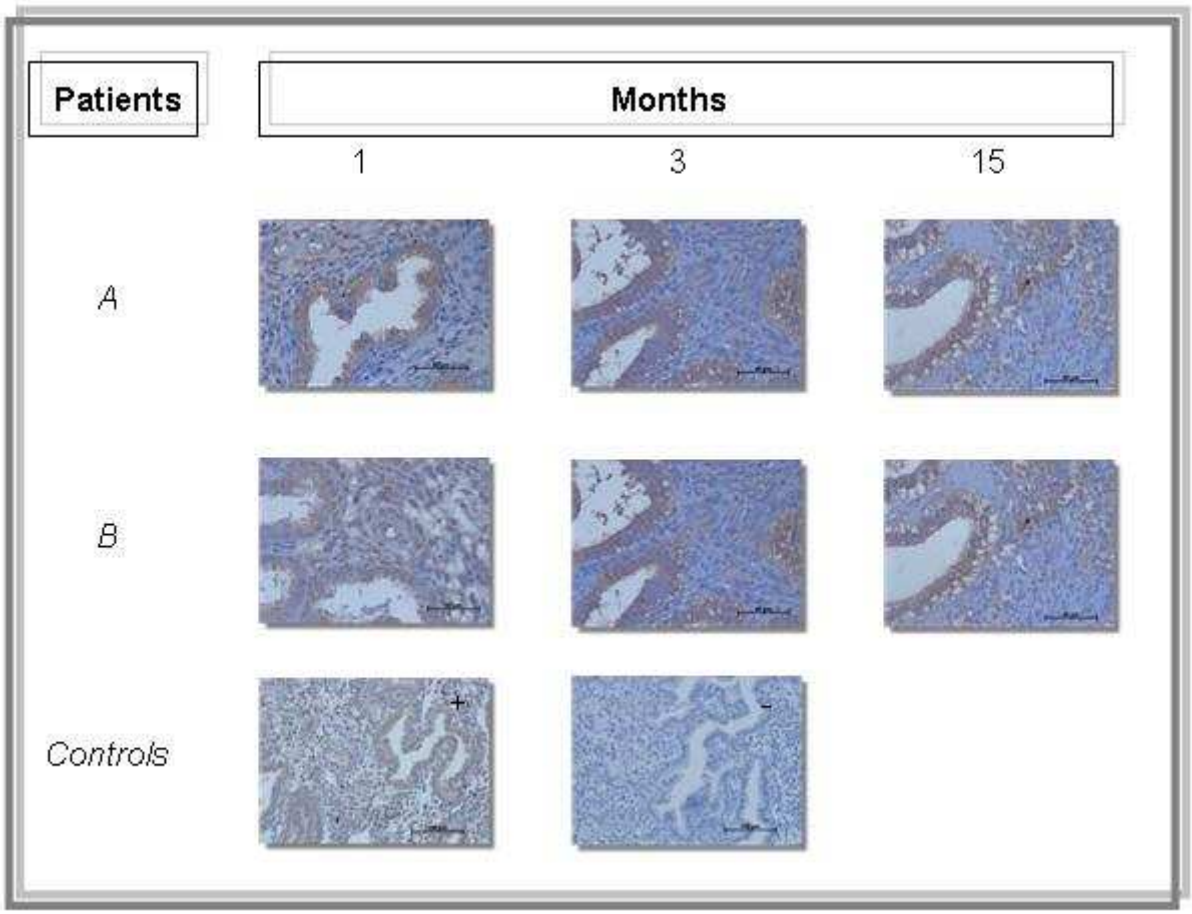

Figure 18: Immunohistochemical analysis of paraffin-embedded endometrium sections of patients A and B. Temporal expression and localisation of prokineticin 1 (PROK-1) was detected at the mid-secretory phase. Staining decreased in glands and stroma as the duration of IUD exposure increased (magnification 50 µm).

We show the results of expression of PROK-1 in the following table (Table 6).

PATIENTS	SLIDES	Gland	Stroma	Vessels/endotelium	Epithelial Surface	Nucl(N)/cyto Gland (G)/Stro (S)	Secreted
A	A,1	++	++	+	++	GC SN	+
	A,2	+	+	-	+	GC SN	++
	A,3a	+	+	-	+	GC SC/N	++
	A,3b	+	+	-	+	GC SC	++
B	B,1	++	++	+	+	GC SC/N	++
	B,2	++	++	+	-	GC SC/N	++
	B,3	++	++	+	-	GC SC/N	++
C	C,1	++	++	+	-	GC SC/N	+
	C,2	0	0	0	0	0	0
	C,3	+	++	+	-	GC SC/N	+
Positive controls	MS	++	++	++	++	GC SC/N	+
	P	++	++	++	0	GNC SN	++
Negative controls	Rabbit IgG	+/-	+/-	+/-	+	GN SN	+
	Neg no Ab	-	-	-	-	-	-

Table 6: Designations of – (negative), +/- (weakly positive), ++ (strongly positive) and 0 (invaluable result) indicate the relative intensities of the signals. Patients are designated as samples A, B and C. P (proliferative phase) and MS (mid-secretory phase) are positive controls. We used two negative controls. In one of them, we did not use primary antibody (Neg no Ab), and in the other control we used rabbit IgG.

Prokineticin 1 Receptor (PROK-R1)

Glandular cytoplasm, nuclei and cytoplasm of stromal cells also displayed immunoreactivity for PROK-R1. A slight decrease in the stroma and glandular staining was detected in the samples after IUD insertion compared with samples taken before and during IUD placement in the same patients (Fig. 19).

Neither rabbit IgG nor the negative control with no primary antibody showed staining, whereas both positive controls were completely positive.

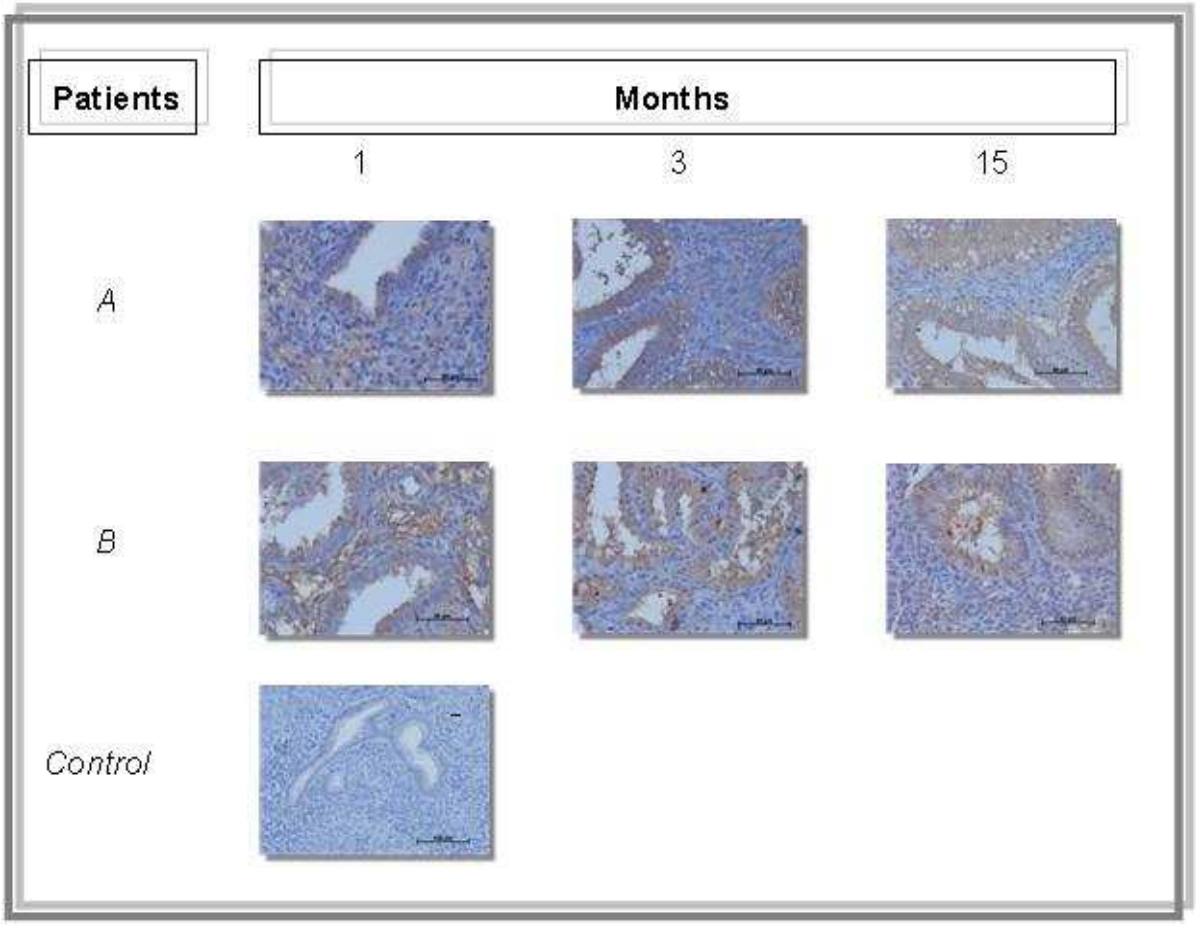

Figure 19: Immunohistochemical analysis of paraffin-embedded endometrium sections from patients A and B. Temporal expression and localisation of the prokineticin 1 receptor (PROK-R1) was detected at the mid-secretory phase. Endometrial biopsies were obtained before, during and after IUD placement, respectively at months 1 (A1/B1), 3 (A2/B2) and 15 (A3/B3). The result of the negative control for PROK-R1 using rabbit IgG is completely negative. For antibody dilutions, see the Materials and Methods section.

The summary of the results is presented in the table below (Table 7):

PATIENTS	SLIDES	Glands	Stroma	Vessels/endotelium	Epithelial Surface	Nucl(N)/cyto Gland (G)/Stro (S)	Secreted
A	A,1	++	++	-	+	GC SNC	-
	A,2	+	+	-	+	GC SNC	+
	A,3a	+	+	-	-	GC SNC	-
	A,3b	+	+	-	+	GC SNC	++
B	B,1	++	++	-	-	GC SNC	+
	B,2	++	+	+	-	GC SNC	+
	B,3	++	+	-	+	GC SNC	+
C	C,1	+	++	-	-	GC SNC	+
	C,2	0	0	0	0	0	0
	C,3	+	+	-	-	GC SNC	+
Positive controls	MS	++	++	++	++	GC SC/N	+
	P	++	++	++	0	GNC SN	++
Negative controls	Rabbit IgG	-	-	-	-	-	-
	Neg no Ab	-	-	-	-	-	-

Table 7: Designations of – (negative), + (weakly positive), ++ (strongly positive) and 0 (invaluable result) indicate the relative intensities of the signals.

Immunohistochemical localisation of LIF.

To investigate the potential endometrial regulation of LIF by the IUD, we tested two concentrations (1:50 and 1:25); the results shown correspond to the 1:25 dilution. The staining pattern was localised in the glandular cytoplasm and nuclei of stroma cells. Stroma staining decreased at month 3, but at month 15 the staining was as high as in the samples before IUD insertion.

Among the differences found, we can mention decreased staining in vessels and on the epithelial surface during (month 3) and after IUD placement (month 15) with respect to the biopsies before IUD insertion (month 1). The signal in the negative control was slightly positive, probably because the antibody used may be non-specific; nevertheless, there was a

clear reduction in staining of this control compared with the study samples (Fig. 20).

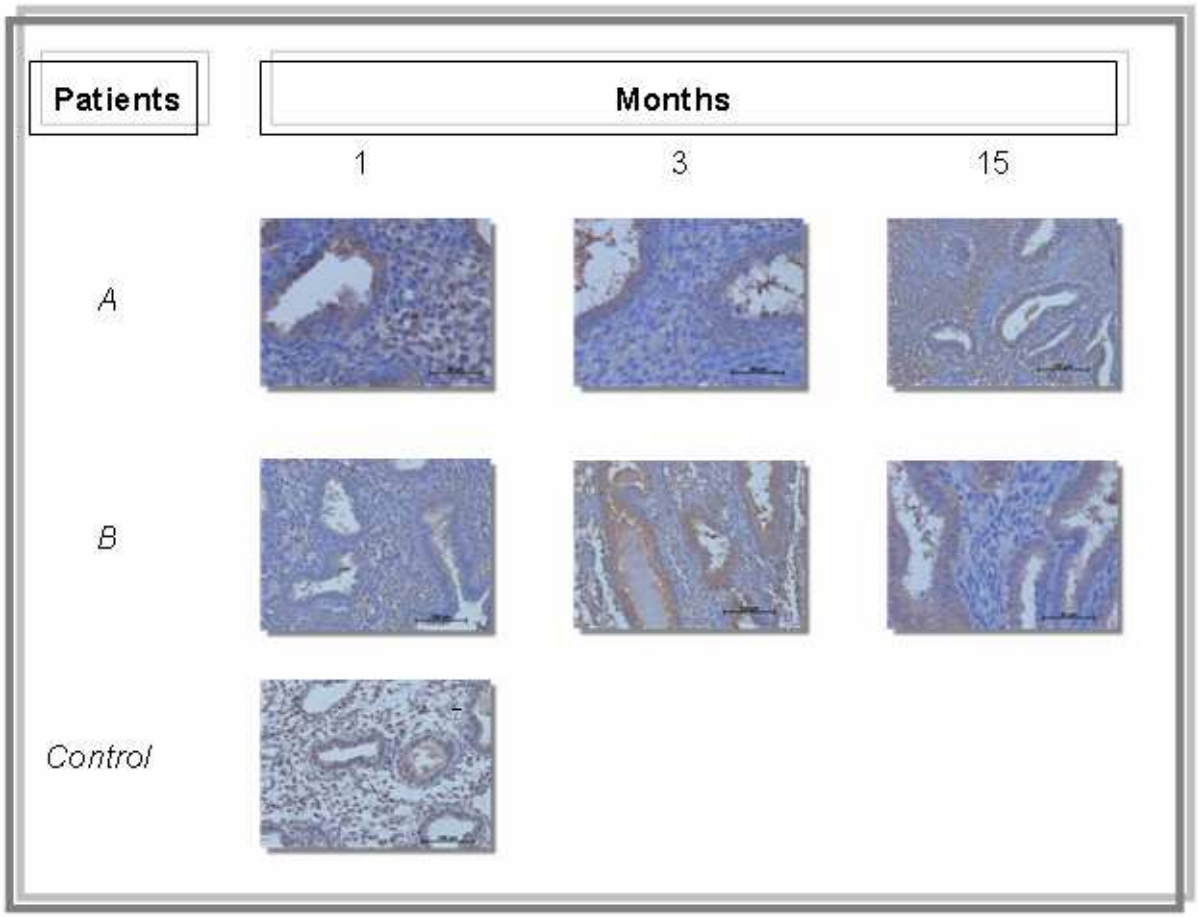

Figure 20: Immunohistochemical analysis of paraffin-embedded endometrium sections from patients A and B. Temporal expression and localisation of leukaemia inhibitory factor (LIF) was detected at the mid-secretory phase. Endometrial biopsies were obtained before, during and after IUD placement, respectively, at months 1, 3 and 15. Staining decreased in the stroma at month 3 but increased again in samples after IUD exposure at month 15. For antibody dilutions, see the Materials and Methods section.

We present the summary of results for LIF in Table 8.

PATIENTS	SLIDES	Glands	Stroma	Vessels/endotelium	Epithelial Surface	Nucl(N)/cyto Gland (G)/Stro (S)	Secreted
A	A,1	++	++	+	++	GC SN	+
	A,2	++	+	+	++	GC SN	++
	A,3a	++	++	-	-	GC SN	++
	A,3b	++	++	+	+	GC SN	++
B	B,1	++	++	+	+	GC SN	++
	B,2	++	+	+	+	GC SN	++
	B,3	++	+	+	+	GC SN	++
C	C,1	++	++	++	+	GC SN	++
	C,2	0	0	0	0	0	0
	C,3	++	++	+	+/-	GC SN	++
Positive controls	MS	++	++	++	++	GC SN	-
	P	++	++	++	++	GCN / SN	+
Negative control	Goat IgG	+	+	+	++	GCN / SN	-

Table 8: Designations of – (negative), + (weakly positive), ++ (strongly positive) and 0 (invaluable result) indicate the relative intensities of the signals. Patients are designated as samples A, B and C. P (proliferative phase) and MS (mid-secretory phase) are positive controls. The negative control used is Goat IgG.

6. DISCUSSION

This study demonstrated the clinical safety, stability and tolerance of the implantation and retrieval of the unloaded Anecova device in the uterus for a period of up to 6 days. Furthermore, we investigated the genomic impact of the device on the endometrium, compared with control endometrium without implantation of the device, at day hCG+7 in ovum donors undergoing IVF in whom this device was inserted for one, three or five days prior to endometrial biopsy.

The hysteroscopic evaluation in volunteer oocyte donors who had the Anecova device implanted for 24 hours or 6 days did not show relevant macroscopic differences. There were no signs of inflammatory changes such as hyperaemia, strawberry pattern, or hypervascularisation [95]. This absence of disorders is reassuring from a macroscopic point of view. In addition, our findings make a useful contribution to future studies, including improvements in the device's design. Improvements will be necessary because the device was displaced further into the isthmus in three patients, and in another patient it was displaced the day after its insertion. These findings suggest that a sterile tampon should be placed into the vagina to maintain the placement of the device in future studies.

Our data on the effect of the new Anecova device on the endometrium revealed no differences in the global gene expression profiles between specimens, regardless of the duration of insertion. Our patients were allocated into 4 groups (n=5 per group), and the Anecova device was inserted

for 18 hours, 3 days or 5 days, or not at all as a control, after oocyte retrieval.

Few dysregulated genes were observed in the 3-day group that were related to specific cellular functions, such as metabolic processes, gamma-glutamyltransferase activity, arachidonic-acid metabolism and glutathione metabolism. Gamma-glutamyltransferase is related to glutathione metabolism by transferring the glutamylmoiety to a variety of acceptor molecules [96]. The arachidonic-acid metabolism produces signalling molecules called eicosanoids, which include prostaglandins, leukotrienes and lipoxins [97]. All of these molecules control key cellular processes, including cell activation, metabolism, migration, proliferation and death [98, 99].

Among glutathione's functions are detoxification, antioxidant defence, maintenance of thiol status involved in cell death and modulation of cell proliferation [100]. In addition, the intracellular antioxidant system based on glutathione could be involved in the pathogenesis of endometriosis [101].

These findings suggest a possible inflammatory reaction of the endometrium to the presence of a foreign body, but no clear differences were found after clustering or PCA analysis.

To test the impact of this new device on the endometrium compared with a regular IUD, we conducted an immunohistochemistry control study analysing three distinct molecules: PRs, PROK-1 and PROK-1R, that are key

molecules for endometrial receptivity.

In the analysis of progesterone receptors (PR), we chose an antibody that binds to both receptors (PRA and PRB) according to previously published studies [102]. Our findings in control samples during the proliferative phase are consistent with those observed by Mote's team some years ago [72]. Levels of PR proteins were increased in glands and stroma, probably because of estrogen stimulation in the glandular epithelium during the proliferative phase.

Our results do not show a significant change in the expression of PR due to the IUD either during its use or one year after its removal. The expression of PR was very similar across the three insertion durations in both glands and stroma cells, showing very weak staining.

Other authors, such as Critchley and Zhu, determined the endometrial expression of PR (both receptors) in women who had a levonorgestrel-releasing IUD inserted for a total period of 12–15 months [103, 104]. In both studies, PRA and PRB immunoreactivity showed a statistically significant decrease of PR in the endometrium of users of this type of IUD compared with biopsies prior to insertion of the IUD, but this decrease was neither uniform nor cell-specific.

Our results cannot be compared with theirs for three reasons. First, their data were pooled regardless of cycle phase (in the case of Critchley) or the samples were collected in the proliferative phase (in Zhu's study).

Second, the total time of exposure to the device was approximately one year, whereas in our study the device was inside the uterus for only one month. Finally, both Critchley and Zhu used an IUD loaded with levonorgestrel. This type of IUD can have side effects such as intermenstrual spotting and amenorrhoea, which could cause problems for the patients. The Lippes Loop Intrauterine Double-S, which we used in this work, is not associated with any hormone that could modify the gene expression profile, so it is considered a quite inert device. This feature makes it a good control for the Anecova system.

According to several experiments, the interaction between PROK-1 and PROK-R1 regulates the expression of crucial genes related to the implantation process [105]. Nevertheless, we decided to study PROK-1 instead of PROK-2 because of some results previously reported, such as those obtained by Battersby and collaborators [52]. They hold that PROK-1 can have a regulatory role, whereas PROK-2 may have a permissive function in the uterus. This idea is supported by their PCR data, which indicate a temporal variation in the expression of PROK-1 (high in the secretory phase of the menstrual cycle), but not PROK-2.

Our results for PROK-1 indicate a slight variability among patients. Although, for PROK-R1, we detected a slight decrease in stroma and glandular staining after IUD insertion, we cannot affirm that PROK-1 and PROK-R1 expression is affected by the presence of this type of IUD.

The results obtained from this study are not in total agreement with those reported by Battery's team [52]. They observed a greater expression of PROK-1 during the mid-secretory phase compared with the proliferative phase. This effect is probably mediated via paracrine mechanisms of progesterone, as reported by Kurita and colleagues in in vitro studies in mice [106]. The exact reasons for the differences between these studies and our own are not clear, although they could be attributed to differences in experimental conditions.

We obtained unexpected results for LIF. The commercial antibodies available for this factor are not always comparable, and the purchased antibodies are often non-specific. Therefore, we cannot draw proper conclusions from this experiment.

The global gene expression profile of the endometrium during the window of implantation in the presence or absence of an inert IUD has been described previously [89]. Unlike our results for the endometrial gene expression of the Anecova device, previous research has found significant differences in gene expression due to the presence of this foreign body. The collection of biopsies followed the same protocol as in our study, and the type of IUD used was also the same. Month 1 was a natural cycle before IUD insertion; in month 2, the IUD was inserted; and in month 3, the IUD was removed. The samples were obtained at months 1, 3, 5, and 15.

Biopsies obtained at month 3 showed 78 up-regulated and 69 down-regulated transcripts. When they compared the biopsies collected

after IUD removal with those obtained in the natural cycle, they found interesting results: Only five genes restored their normal expression two months after IUD removal whereas one year later most of the genes (80%) had recovered their normal expression [89].

They identified genes related to apoptosis, ion transporters, immunomodulators, secretory proteins, signal transduction, membrane proteins, and transcription factors. Among these dysregulated genes, they obtained gene expression changes for LIF. This factor, which is usually up-regulated at the time of implantation, was reported to have decreased expression at month 5, although it was restored one year after IUD removal. These findings are consistent with our results for LIF obtained from the immunohistochemistry study.

The hysteroscopic evaluation in volunteer oocyte donors who had the Anecova device implanted for 24 hours or 6 days did not show relevant macroscopic differences. In addition, our findings will contribute to subsequent studies and to improvements in the device's design. In three patients, the device displaced further into the isthmus, and in another patient, it was expelled the day after its insertion. Therefore, we suggest using a sterile tampon placed into the vagina to keep the device in place in future studies.

After ruling out a possible endometrial effect, a pilot study of in vivo embryo development was carried out [107]. The results of this trial are not addressed in this thesis. These results demonstrate that the

embryos introduced using this device divided normally and were chromosomally normal. Furthermore, it was possible to achieve healthy live births after the transient presence of an inert foreign device in the uterus. This was the first work describing a novel in utero culture system that allowed direct communication between the embryos and the maternal endometrium.

One outstanding question is, then, why the Anecova device did not have the same contraceptive effect as the IUDs. One of the potential answers could be that the non-allergenic components of the device (mainly silicone, titanium and suture) prevent the effects of the different materials that are used in the IUDs.

Another possible explanation of the safety of the Anecova device may be the period of time that it remains inside the uterus. In this case, we studied the gene expression changes caused by the insertion of the device for a maximum of 5 days, whereas an IUD can remain inside the uterus for months or years.

Finally, another potential reason for the different effect of the Anecova device is the place of insertion. An IUD must be inserted at the fundus of the uterus, whereas the new system is located in the lower uterine segment. Therefore, it remains to be determined whether different parts of endometrium have distinct gene modulation patterns in response to a similar stimulus.

Although in vivo embryo development studies using this device have already been reported, further studies will clearly be required to confirm the functionality of this new in vivo culture system.

7. CONCLUSIONS

1. The stability of the IUD was acceptable, except in two patients in whom it was displaced further into the isthmus. These findings are useful for directing improvements to the device's design.

2. The hysteroscopic evaluation in volunteers who had the IUD inserted for 24 hours or 6 days did not show relevant macroscopic findings.

3. Wide genomic analysis of the endometrial samples obtained from subjects with the IUD inserted for varying durations reveals no significant differences compared with the controls.

4. Our results do not show a significant change in the expression of PR, PROK-1 or PROK-R1.

5. In summary, we demonstrated the safety and tolerance of the insertion and retrieval of the IUD and the absence of relevant endometrial genetic impact of this unloaded device in the uterus for up to 6 days.

8. ANNEXES

→TABLE 2.1: Device (18 h) Versus Control

UP	p-value	FC	Symbol	Description
AK097517	0,0000	**3,60**	LOC283767	Homo sapiens cDNA FLJ40198 fis, clone TESTI2019975, weakly similar to TRICHOHYALIN. [AK097517]
NM_139172	0,0000	**3,59**	MDAC1	Homo sapiens MDAC1 (MDAC1), mRNA [NM_139172]
XM_498537	0,0033	**3,28**	LOC440084	PREDICTED: Homo sapiens hypothetical LOC440084 (LOC440084), mRNA [XM_498537]
NM_001013680	0,0050	**3,01**	LOC401233	Homo sapiens similar to HIV TAT specific factor 1; cofactor required for Tat activation of HIV-1 transcription (LOC401233), mRNA [NM_001013680]
S82024	0,0040	**2,97**	STMN2	SCG10=neuron-specific growth-associated protein/stathmin homolog [human, embryo, mRNA, 696 nt]. [S82024]
BC020847	0,0125	**2,81**	LOC644246	Homo sapiens hypothetical protein LOC644246, mRNA (cDNA clone IMAGE:4730995), partial cds. [BC020847]
NM_030657	0,0111	**2,80**	LIM2	Homo sapiens lens intrinsic membrane protein 2, 19kDa (LIM2), mRNA [NM_030657]
NM_002423	0,0114	**2,67**	MMP7	Homo sapiens matrix metallopeptidase 7 (matrilysin, uterine) (MMP7), mRNA [NM_002423]
NM_000424	0,0180	**2,53**	KRT5	Homo sapiens keratin 5 (epidermolysis bullosa simplex, Dowling-Meara/Kobner/Weber-Cockayne types) (KRT5), mRNA [NM_000424]
NM_002571	0,0067	**2,27**	PAEP	Homo sapiens progestagen-associated endometrial protein (placental protein 14, pregnancy-associated endometrial alpha-2-globulin, alpha uterine protein) (PAEP), transcript variant 2, mRNA [NM_002571]
DOWN	**p-value**	**FC**	**Symbol**	**Description**
NR_002834	0,0000	**-3,08**	DUSP5P	Homo sapiens dual specificity phosphatase 5 pseudogene (DUSP5P) on chromosome 1 [NR_002834]
BI752712	0,0000	**-2,81**	BI752712	BI752712 603028325F1 NIH_MGC_114 Homo sapiens cDNA clone IMAGE:5198503 5', mRNA sequence [BI752712]
NR_002940	0,0300	**-2,31**	FLJ10120	Homo sapiens hypothetical protein FLJ10120 (FLJ10120) on chromosome 17 [NR_002940]
AK000470	0,0240	**-2,23**	LOC286434	Homo sapiens cDNA FLJ20463 fis, clone KAT06143. [AK000470]
NM_144587	0,0467	**-2,10**	BTBD16	Homo sapiens BTB (POZ) domain containing 16 (BTBD16), mRNA [NM_144587]
M27126	0,0167	**-2,10**	M27126	Human lymphocyte antigen (DRw8) mRNA. [M27126]

Table 2.1 (Results: 4.2.2): This table shows the 10 up- and 6 down-regulated DNA probes in samples obtained after insertion of the device for 18 h compared with the control samples. The table summarises the number of the probes with a fold change larger than 2 or smaller than -2 and a statistical significance lower than 0.05 in all of the mentioned comparisons. The genes are named according to the National Center for Biotechnology Information (NCBI) database.

→TABLE 2.2: Device (3 days) Versus Control

Table 2.2.A:

UP	p value	FC	Symbol	Description
AK124400	0,0000	**4,78**	LOC553137	Homo sapiens cDNA FLJ42409 fis, clone BLADE2000866. [AK124400]
AK055838	0,0000	**4,39**	AK055838	Homo sapiens cDNA FLJ31276 fis, clone KIDNE2006376, weakly similar to GAMMA-GLUTAMYLTRANSPEPTIDASE 1 PRECURSOR (EC 2.3.2.2). [AK055838]
NM_014358	0,0000	**3,75**	CLEC4E	Homo sapiens C-type lectin domain family 4, member E (CLEC4E), mRNA [NM_014358]
NM_080920	0,0014	**3,57**	GGTLA4	Homo sapiens gamma-glutamyltransferase-like activity 4 (GGTLA4), transcript variant C, mRNA [NM_080920]
NM_139172	0,0020	**3,43**	MDAC1	Homo sapiens MDAC1 (MDAC1), mRNA [NM_139172]
XM_498537	0,0008	**3,41**	LOC440084	PREDICTED: Homo sapiens hypothetical LOC440084 (LOC440084), mRNA [XM_498537]
NM_021046	0,0000	**3,31**	KRTAP5-8	Homo sapiens keratin associated protein 5-8 (KRTAP5-8), mRNA [NM_021046]
AK097517	0,002700	**3,17**	LOC283767	Homo sapiens cDNA FLJ40198 fis, clone TESTI2019975, weakly similar to TRICHOHYALIN. [AK097517]
NM_002571	0,0031	**3,10**	PAEP	Homo sapiens progestagen- associated endometrial protein (placental protein 14, pregnancy-associated endometrial alpha-2- globulin, alpha uterine protein) (PAEP), transcript variant 2, mRNA [NM_002571]
NM_002084	0,0060	**3,04**	GPX3	Homo sapiens glutathione peroxidase 3 (plasma) (GPX3), mRNA [NM_002084]
NM_000558	0,0017	**3,02**	HBA1	Homo sapiens hemoglobin, alpha 1 (HBA1), mRNA [NM_000558]
AB016898	0,0011	**2,97**	LOC653483	Homo sapiens HGC6.4 mRNA, complete cds. [AB016898]
NM_006439	0,0010	**2,96**	MAB21L2	Homo sapiens mab -21-like 2 (C. elegans) (MAB21L2), mRNA [NM_006439]
XR_015191	0,0061	**2,91**	LOC728044	PREDICTED: Homo sapiens similar to immunoglobulin superfamily, member 3 isoform 2 (LOC728044), mRNA [XR_015191]
NR_003267	0,0015	**2,86**	GGT2	Homo sapiens gamma-glutamyltransferase 2 (GGT2) on chromosome 22 [NR_003267]
NM_005252	0,0013	**2,83**	FOS	Homo sapiens v- fos FBJ murine osteosarcoma viral oncogene homolog (FOS), mRNA [NM_005252]
NM_006744	0,0166	**2,80**	RBP4	Homo sapiens retinol binding protein 4, plasma (RBP4), mRNA [NM_006744]

NM_080621	0,0047	**2,78**	SAMD10	Homo sapiens sterile alpha motif domain containing 10 (SAMD10), mRNA [NM_080621]
NM_001718	0,0108	**2,61**	BMP6	Homo sapiens bone morphogenetic protein 6 (BMP6), mRNA [NM_001718]
NM_173502	0,0009	**2,56**	PRSS36	Homo sapiens protease, serine, 36 (PRSS36), mRNA [NM_173502]
NM_001770	0,0100	**2,48**	CD19	Homo sapiens CD19 molecule (CD19), mRNA [NM_001770]
NM_000517	0,0067	**2,48**	HBA2	Homo sapiens hemoglobin, alpha 2 (HBA2), mRNA [NM_000517]
NM_001017402	0,0290	**2,44**	LAMB3	Homo sapiens laminin, beta 3 (LAMB3), transcript variant 2, mRNA [NM_001017402]
BC064586	0,0242	**2,43**	LOC145837	Homo sapiens hypothetical protein LOC145837, mRNA (cDNA clone IMAGE:5740791), partial cds. [BC064586]
BC104421	0,0164	**2,42**	BC104421	Homo sapiens cDNA clone IMAGE:40004940. [BC104421]
NM_001159	0,0113	**2,42**	AOX1	Homo sapiens aldehyde oxidase 1 (AOX1), mRNA [NM_001159]
NM_005265	0,0162	**2,40**	GGT1	Homo sapiens gamma- glutamyltransferase 1 (GGT1), transcript variant 1, mRNA [NM_005265]
NM_031451	0,0234	**2,38**	TEX101	Homo sapiens testis expressed sequence 101 (TEX101), mRNA [NM_031451]
NM_002888	0,0304	**2,34**	RARRES1	Homo sapiens retinoic acid receptor responder (tazarotene induced) 1 (RARRES1), transcript variant 2, mRNA [NM_002888]
NM_020396	0,0302	**2,34**	BCL2L10	Homo sapiens BCL2- like 10 (apoptosis facilitator) (BCL2L10), mRNA [NM_020396]
NM_145659	0,0021	**2,32**	IL27	Homo sapiens interleukin 27 (IL27), mRNA [NM_145659]
NM_144669	0,0322	**2,30**	GLT1D1	Homo sapiens glycosyltransferase 1 domain containing 1 (GLT1D1), mRNA [NM_144669]
NM_052952	0,0058	**2,30**	DIRC1	Homo sapiens disrupted in renal carcinoma 1 (DIRC1), mRNA [NM_052952]
NM_001024465	0,0345	**2,30**	SOD2	Homo sapiens superoxide dismutase 2, mitochondrial (SOD2), nuclear gene encoding mitochondrial protein, transcript variant 2, mRNA [NM_001024465]
DQ655984	0,0124	**2,30**	DQ655984	Homo sapiens clone Affy08248C01, mRNA sequence. [DQ655984]

NM_005564	0,0295	**2,29**	LCN2	Homo sapiens lipocalin 2 (oncogene 24p3) (LCN2), mRNA [NM_005564]
NM_021966	0,0237	**2,28**	TCL1A	Homo sapiens T-cell leukemia/lymphoma 1A (TCL1A), mRNA [NM_021966]
NM_199127	0,0239	**2,24**	GGTL4	Homo sapiens gamma-glutamyltransferase-like 4 (GGTL4), transcript variant 1, mRNA [NM_199127]
XM_929703	0,0273	**2,22**	LOC646753	PREDICTED: Homo sapiens similar to 40S ribosomal protein S26 (LOC646753), mRNA [XM_929703]
BX161420	0,0241	**2,22**	IGHM	human full-length cDNA clone CS0DD006YL02 of Neuroblastoma of Homo sapiens (human). [BX161420]
AJ276555	0,0300	**2,20**	AJ276555	Homo sapiens mRNA for hypothetical protein (ORF1), clone 00275. [AJ276555]
BC021053	0,0343	**2,20**	BC021053	Homo sapiens cDNA clone IMAGE:2960979, **** WARNING: chimeric clone ****. [BC021053]
NM_000361	0,0342	**2,19**	THBD	Homo sapiens thrombomodulin (THBD), mRNA [NM_000361]
ENST00000327591	0,0307	**2,17**	ENST00000327591	Ribosomal protein S26 (Fragment). [Source:Uniprot/SPTREMBL;Acc:Q76N57] [ENST00000327591]
NM_021114	0,0310	**2,17**	SPINK2	Homo sapiens serine peptidase inhibitor, Kazal type 2 (acrosin-trypsin inhibitor) (SPINK2), mRNA [NM_021114]
NM_024764	0,0348	**2,17**	C14orf161	Homo sapiens chromosome 14 open reading frame 161 (C14orf161), mRNA [NM_024764]
NM_005309	0,0281	**2,14**	GPT	Homo sapiens glutamic-pyruvate transaminase (alanine aminotransferase) (GPT), mRNA [NM_005309]
BM129308	0,0428	**2,14**	BM129308	if20d02.x1 Melton Normalized Human Islet 4 N4-HIS 1 Homo sapiens cDNA clone IMAGE:5677082 3', mRNA sequence [BM129308]
ENST00000339425	0,0344	**2,13**	ENST00000339425	C21orf81 protein. [Source:Uniprot/SPTREMBL;Acc:Q49A76] [ENST00000339425]
NM_013322	0,0423	**2,11**	SNX10	Homo sapiens sorting nexin 10 (SNX10), mRNA [NM_013322]
NM_006732	0,0159	**2,10**	FOSB	Homo sapiens FBJ murine osteosarcoma viral oncogene homolog B (FOSB), mRNA [NM_006732]
NM_139072	0,0312	**2,10**	DNER	Homo sapiens delta/notch-like EGF repeat containing (DNER), mRNA [NM_139072]
ENST00000381655	0,0305	**2,09**	ENST00000381655	Probable phospholipid-transporting ATPase IB (EC 3.6.3.1) (ATPase class I type 8A member 2) (ML-1). [ENST00000381655]
NM_000349	0,0352	**2,06**	STAR	Homo sapiens steroidogenic acute regulator (STAR), nuclear gene encoding mitochondrial protein, transcript variant 1, mRNA [NM_000349]
M26004	0,0395	**2,06**	CR2	Human CR2/CD21/C3d/Epstein-Barr virus receptor mRNA, complete cds. [M26004]
NM_000518	0,0482	**2,04**	HBB	Homo sapiens hemoglobin, beta (HBB), mRNA [NM_000518]
ENST00000339446	0,0412	**2,02**	LOC387763	Homo sapiens hypothetical LOC387763, mRNA (cDNA clone IMAGE:6272440), partial cds. [BC052560]

Table 2.2.B:

DOWN	p-value	FC	Symbol	Description
NM_006952	0,0000	**-5,05**	UPK1B	Homo sapiens uroplakin 1B (UPK1B), mRNA [NM_006952]
NM_057157	0,0000	**-4,74**	CYP26A1	Homo sapiens cytochrome P450, family 26, subfamily A, polypeptide 1 (CYP26A1), transcript variant 2, mRNA [NM_057157]
NM_004173	0,0000	**-4,20**	SLC7A4	Homo sapiens solute carrier family 7 (cationic amino acid transporter, y+ system), member 4 (SLC7A4), mRNA [NM_004173]
NM_021801	0,0121	**-4,15**	MMP26	Homo sapiens matrix metallopeptidase 26 (MMP26), mRNA [NM_021801]
NM_014289	0,0000	**-3,47**	CAPN6	Homo sapiens calpain 6 (CAPN6), mRNA [NM_014289]
NM_015686	0,0020	**-3,46**	TMEM28	Homo sapiens transmembrane protein 28 (TMEM28), mRNA [NM_015686]
ENST00000322839	0,0011	**-3,21**	ENST00000322839	Numb- interacting protein [Source: RefSeq peptide; Acc: NP_653166] [ENST00000322839]
NM_017434	0,0058	**-3,15**	DUOX1	Homo sapiens dual oxidase 1 (DUOX1), transcript variant 1, mRNA [NM_017434]
NM_178536	0,0050	**-3,13**	LCN12	Homo sapiens lipocalcin 12 (LCN12), mRNA [NM_178536]
NM_002758	0,0014	**-3,11**	MAP2K6	Homo sapiens mitogen- activated protein kinase kinase 6 (MAP2K6), mRNA [NM_002758]
NM_144705	0,0017	**-3,10**	TEKT4	Homo sapiens tektin 4 (TEKT4), mRNA [NM_144705]
NM_001033515	0,0054	**-3,00**	LOC389833	Homo sapiens similar to hypothetical protein MGC27019 (LOC389833), mRNA [NM_001033515]
NM_000624	0,0138	**-2,96**	SERPINA5	Homo sapiens serpin peptidase inhibitor, clade A (alpha-1 antiproteinase, antitrypsin), member 5 (SERPINA5), mRNA [NM_000624]
NM_177531	0,0056	**-2,84**	PKHD1L1	Homo sapiens polycystic kidney and hepatic disease 1 (autosomal recessive)-like 1 (PKHD1L1), mRNA [NM_177531]
NM_004389	0,0059	**-2,82**	CTNNA2	Homo sapiens catenin (cadherin-associated protein), alpha 2 (CTNNA2), mRNA [NM_004389]
AK126241	0,0134	**-2,82**	FLJ44253	Homo sapiens cDNA FLJ44253 fis, clone TKIDN2009092. [AK126241]
BC037328	0,0063	**-2,76**	BC037328	Homo sapiens cDNA clone IMAGE:5263455. [BC037328]
NM_022746	0,0126	**-2,72**	MOSC1	Homo sapiens MOCO sulphurase C-terminal domain containing 1 (MOSC1), mRNA [NM_022746]
CR613736	0,0123	**-2,71**	CR613736	full-length cDNA clone CS0DI072YA21 of Placenta Cot 25-normalized of Homo sapiens (human). [CR613736]
NM_198277	0,0129	**-2,71**	SLC37A2	Homo sapiens solute carrier family 37 (glycerol-3-phosphate transporter), member 2 (SLC37A2), mRNA [NM_198277]
NM_003280	0,0153	**-2,71**	TNNC1	Homo sapiens troponin C type 1 (slow) (TNNC1), mRNA [NM_003280]
BC068588	0,0060	**-2,69**	LOC653071	Homo sapiens similar to CG32820-PA, isoform A, mRNA (cDNA clone IMAGE:4812880), with apparent retained intron. [BC068588]
NM_025087	0,0132	**-2,68**	FLJ21511	Homo sapiens hypothetical protein FLJ21511 (FLJ21511), mRNA [NM_025087]
NM_000487	0,0050	**-2,66**	ARSA	Homo sapiens arylsulfatase A (ARSA), mRNA [NM_000487]

XR_018597	0,0155	**-2,62**	LOC649344	PREDICTED: Homo sapiens similar to Keratin, type II cytoskeletal 8 (Cytokeratin-8) (CK-8) (Keratin-8) (K8) (LOC649344), mRNA [XR_018597]
NM_001615	0,0136	**-2,62**	ACTG2	Homo sapiens actin, gamma 2, smooth muscle, enteric (ACTG2), mRNA [NM_001615]
XM_001125792	0,0045	**-2,60**	LOC727834	PREDICTED: Homo sapiens hypothetical protein LOC727834 (LOC727834), mRNA [XM_001125792]
NM_015515	0,0208	**-2,58**	KRT23	Homo sapiens keratin 23 (histone deacetylase inducible) (KRT23), mRNA [NM_015515]
NM_032387	0,0133	**-2,57**	WNK4	Homo sapiens WNK lysine deficient protein kinase 4 (WNK4), mRNA [NM_032387]
NM_014553	0,0203	**-2,57**	TFCP2L1	Homo sapiens transcription factor CP2-like 1 (TFCP2L1), mRNA [NM_014553]
ENST00000222543	0,0308	**-2,57**	TFPI2	Tissue factor pathway inhibitor 2 precursor (TFPI-2) (Placental protein 5) (PP5). [Source:Uniprot/SWISSPROT;Acc:P48307] [ENST00000222543]
NM_000440	0,0233	**-2,57**	PDE6A	Homo sapiens phosphodiesterase 6A, cGMP-specific, rod, alpha (PDE6A), mRNA [NM_000440]
NM_005021	0,0291	**-2,56**	ENPP3	Homo sapiens ectonucleotide pyrophosphatase/phosphodiesterase 3 (ENPP3), mRNA [NM_005021]
NM_005769	0,0250	**-2,54**	CHST4	Homo sapiens carbohydrate (N-acetylglucosamine 6-O) sulfotransferase 4 (CHST4), mRNA [NM_005769]
NM_018214	0,0282	**-2,52**	LRRC1	Homo sapiens leucine rich repeat containing 1 (LRRC1), mRNA [NM_018214]
XR_018641	0,0210	**-2,51**	LOC649545	PREDICTED: Homo sapiens similar to Keratin, type II cytoskeletal 8 (Cytokeratin-8) (CK-8) (Keratin-8) (K8) (LOC649545), mRNA [XR_018641]
XR_018415	0,0233	**-2,49**	LOC402429	PREDICTED: Homo sapiens similar to Keratin, type II cytoskeletal 8 (Cytokeratin-8) (CK-8) (Keratin-8) (K8) (LOC402429), mRNA [XR_018415]
M27126	0,0013	**-2,47**	M27126	Human lymphocyte antigen (DRw8) mRNA. [M27126]
NM_016725	0,0185	**-2,46**	FOLR1	Homo sapiens folate receptor 1 (adult) (FOLR1), transcript variant 1, mRNA [NM_016725]
NM_001321	0,0270	**-2,44**	CSRP2	Homo sapiens cysteine and glycine-rich protein 2 (CSRP2), mRNA [NM_001321]
AL109695	0,0208	**-2,43**	AL109695	Homo sapiens mRNA full length insert cDNA clone EUROIMAGE 39820. [AL109695]
NM_033051	0,0191	**-2,42**	TSCOT	Homo sapiens thymic stromal co-transporter (TSCOT), mRNA [NM_033051]
NM_032446	0,0256	**-2,38**	MEGF10	Homo sapiens multiple EGF-like-domains 10 (MEGF10), mRNA [NM_032446]
XR_019203	0,0292	**-2,38**	LOC390472	PREDICTED: Homo sapiens similar to Keratin, type II cytoskeletal 8 (Cytokeratin-8) (CK-8) (Keratin-8) (K8) (LOC390472), mRNA [XR_019203]
XR_017139	0,0295	**-2,35**	LOC342419	PREDICTED: Homo sapiens similar to Keratin, type II cytoskeletal 8 (Cytokeratin-8) (CK-8) (Keratin-8) (K8) (Cytokeratin endo A) (LOC342419), mRNA [XR_017139]
AK096051	0,0302	**-2,33**	LOC348174	Homo sapiens cDNA FLJ38732 fis, clone KIDNE2010750. [AK096051]
NM_173160	0,0365	**-2,33**	FXYD4	Homo sapiens FXYD domain containing ion transport regulator 4 (FXYD4), mRNA [NM_173160]
NM_004004	0,0120	**-2,31**	GJB2	Homo sapiens gap junction protein, beta 2, 26kDa (connexin 26) (GJB2), mRNA [NM_004004]
NM_001248	0,0300	**-2,28**	ENTPD3	Homo sapiens ectonucleoside triphosphate diphosphohydrolase 3 (ENTPD3), mRNA [NM_001248]

NM_005797	0,0411	-2,28	EVA1	Homo sapiens epithelial V-like antigen 1 (EVA1), transcript variant 1, mRNA [NM_005797]
NM_021115	0,0487	-2,27	SEZ6L	Homo sapiens seizure related 6 homolog (mouse)-like (SEZ6L), mRNA [NM_021115]
NM_053055	0,0356	-2,26	THEM4	Homo sapiens thioesterase superfamily member 4 (THEM4), mRNA [NM_053055]
NM_017662	0,0384	-2,25	TRPM6	Homo sapiens transient receptor potential cation channel, subfamily M, member 6 (TRPM6), mRNA [NM_017662]
NM_001010926	0,0346	-2,25	HES5	Homo sapiens hairy and enhancer of split 5 (Drosophila) (HES5), mRNA [NM_001010926]
XR_018299	0,0384	-2,24	LOC347333	PREDICTED: Homo sapiens similar to Keratin, type II cytoskeletal 8 (Cytokeratin-8) (CK-8) (Keratin-8) (K8) (LOC347333), mRNA [XR_018299]
NM_001040153	0,0450	-2,23	SLAIN1	Homo sapiens SLAIN motif family, member 1 (SLAIN1), transcript variant 1, mRNA [NM_001040153]
NM_001040708	0,0353	-2,22	HEY1	Homo sapiens hairy/enhancer-of-split related with YRPW motif 1 (HEY1), transcript variant 2, mRNA [NM_001040708]
NM_001165	0,0298	-2,21	BIRC3	Homo sapiens baculoviral IAP repeat-containing 3 (BIRC3), transcript variant 1, mRNA [NM_001165]
NM_172082	0,0378	-2,20	CAMK2B	Homo sapiens calcium/calmodulin-dependent protein kinase (CaM kinase) II beta (CAMK2B), transcript variant 6, mRNA [NM_172082]
AK094356	0,0443	-2,19	LOC286382	Homo sapiens cDNA FLJ37037 fis, clone BRACE2011611. [AK094356]
NM_000775	0,0265	-2,19	CYP2J2	Homo sapiens cytochrome P450, family 2, subfamily J, polypeptide 2 (CYP2J2), mRNA [NM_000775]
NM_022910	0,0191	-2,19	NDRG4	Homo sapiens NDRG family member 4 (NDRG4), mRNA [NM_022910]
NM_002252	0,0318	-2,18	KCNS3	Homo sapiens potassium voltage-gated channel, delayed-rectifier, subfamily S, member 3 (KCNS3), mRNA [NM_002252]
AB032983	0,0350	-2,17	PPM1H	Homo sapiens mRNA for KIAA1157 protein, partial cds. [AB032983]
NM_000112	0,0365	-2,15	SLC26A2	Homo sapiens solute carrier family 26 (sulfate transporter), member 2 (SLC26A2), mRNA [NM_000112]
NM_001888	0,0292	-2,15	CRYM	Homo sapiens crystallin, mu (CRYM), transcript variant 1, mRNA [NM_001888]
NM_000424	0,0465	-2,15	KRT5	Homo sapiens keratin 5 (epidermolysis bullosa simplex, Dowling-Meara/Kobner/Weber-Cockayne types) (KRT5), mRNA [NM_000424]
NM_002083	0,0280	-2,14	GPX2	Homo sapiens glutathione peroxidase 2 (gastrointestinal) (GPX2), mRNA [NM_002083]
NM_032413	0,0248	-2,14	C15orf48	Homo sapiens chromosome 15 open reading frame 48 (C15orf48), transcript variant 2, mRNA [NM_032413]
NM_021972	0,0095	-2,14	SPHK1	Homo sapiens sphingosine kinase 1 (SPHK1), transcript variant 1, mRNA [NM_021972]
NM_032229	0,0448	-2,14	SLITRK6	Homo sapiens SLIT and NTRK-like family, member 6 (SLITRK6), mRNA [NM_032229]
NM_020789	0,0408	-2,11	IGSF9	Homo sapiens immunoglobulin superfamily, member 9 (IGSF9), mRNA [NM_020789]
BC022881	0,0209	-2,10	LOC644450	Homo sapiens hypothetical protein LOC644450, mRNA (cDNA clone IMAGE:4606942), partial cds. [BC022881]
NM_001676	0,0227	-2,08	ATP12A	Homo sapiens ATPase, H+/K+ transporting, nongastric, alpha polypeptide (ATP12A), mRNA [NM_001676]
AF338232	0,0415	-2,08	CTAGE4	Homo sapiens CTAGE-4 protein mRNA, complete cds. [AF338232]
CR936791	0,0485	-2,06	CR936791	Homo sapiens mRNA; cDNA DKFZp781C2356 (from clone DKFZp781C2356). [CR936791]
AK098064	0,0208	-2,03	CLDN22	Homo sapiens cDNA FLJ40745 fis, clone TRACH2000287, weakly similar to CLAUDIN-6. [AK098064]
NM_022097	0,0437	-2,00	LOC63928	Homo sapiens hepatocellular carcinoma antigen gene 520 (LOC63928), mRNA [NM_022097]

Tables 2.2A/2.2B (Results: 4.2.2): These tables show the data of samples obtained after insertion of the device for 3 days compared with the control samples and summarises the number of probes with a fold change greater than 2 (Table 2.2.A) or less than -2 (Table 2.2.B) and statistical significance lower than 0.05. The genes are named according to the database of the National Center for Biotechnology Information (NCBI).

→TABLE 2.3: Device (5 days) Versus Control

UP	p-value	FC	Symbol	Description
NM_139172	0,0000	**7,09**	MDAC1	Homo sapiens MDAC1 (MDAC1), mRNA [NM_139172]
NM_005252	0,0000	**3,58**	FOS	Homo sapiens v-fos FBJ murine osteosarcoma viral oncogene homolog (FOS), mRNA [NM_005252]
NM_001511	0,0140	**3,09**	CXCL1	Homo sapiens chemokine (C-X-C motif) ligand 1 (melanoma growth stimulating activity, alpha) (CXCL1), mRNA [NM_001511]
NM_000170	0,0233	**2,99**	GLDC	Homo sapiens glycine dehydrogenase (decarboxylating) (GLDC), mRNA [NM_000170]
NM_000558	0,0183	**2,86**	HBA1	Homo sapiens hemoglobin, alpha 1 (HBA1), mRNA [NM_000558]
NM_005573	0,0400	**2,59**	LMNB1	Homo sapiens lamin B1 (LMNB1), mRNA [NM_005573]
NM_002964	0,0214	**2,57**	S100A8	Homo sapiens S100 calcium binding protein A8 (S100A8), mRNA [NM_002964]
XM_001131389	0,0300	**2,51**	LOC730999	PREDICTED: Homo sapiens hypothetical protein LOC730999 (LOC730999), mRNA [XM_001131389]
NM_004062	0,0370	**2,48**	CDH16	Homo sapiens cadherin 16, KSP-cadherin (CDH16), mRNA [NM_004062]
NM_006732	0,0175	**2,44**	FOSB	Homo sapiens FBJ murine osteosarcoma viral oncogene homolog B (FOSB), mRNA [NM_006732]
AK097517	0,0345	**2,40**	LOC283767	Homo sapiens cDNA FLJ40198 fis, clone TESTI2019975, weakly similar to TRICHOHYALIN. [AK097517]
DOWN	**p-value**	**FC**	**Symbol**	**Description**
NM_002411	0,0100	**-2,71**	SCGB2A2	Homo sapiens secretoglobin, family 2A, member 2 (SCGB2A2), mRNA [NM_002411]
AK096051	0,0225	**-2,68**	LOC348174	Homo sapiens cDNA FLJ38732 fis, clone KIDNE2010750. [AK096051]
AK075484	0,0233	**-2,45**	AK075484	Homo sapiens cDNA PSEC0178 fis, clone OVARC1000636, moderately similar to Sterile alpha motif domain containing protein 4. [AK075484]
NM_006846	0,0180	**-2,43**	SPINK5	Homo sapiens serine peptidase inhibitor, Kazal type 5 (SPINK5), mRNA [NM_006846]
NM_144676	0,0167	**-2,34**	TMED6	Homo sapiens transmembrane emp24 protein transport domain containing 6 (TMED6), mRNA [NM_144676]
NM_005807	0,0271	**-2,31**	PRG4	Homo sapiens proteoglycan 4 (PRG4), mRNA [NM_005807]
NM_000663	0,0364	**-2,23**	ABAT	Homo sapiens 4-aminobutyrate aminotransferase (ABAT), nuclear gene encoding mitochondrial protein, transcript variant 2, mRNA [NM_000663]
NM_001062	0,0390	**-2,13**	TCN1	Homo sapiens transcobalamin I (vitamin B12 binding protein, R binder family) (TCN1), mRNA [NM_001062]
NM_005980	0,0288	**-2,06**	S100P	Homo sapiens S100 calcium binding protein P (S100P), mRNA [NM_005980]

Tables 2.3 (Results: 4.2.2): These tables show the data of samples obtained after insertion of the device for 5 days compared with the control samples and summarises the number of probes with a fold change greater than 2 (Table 2.3.A) or less than -2 (Table 2.3.B) and a statistical significance lower than 0.05. The genes are named according to the database of the National Center for Biotechnology Information (NCBI).

9. REFERENCES

1. Steptoe, P.C. and R.G. Edwards, *Birth after the reimplantation of a human embryo.* Lancet, 1978. **2**(8085): p. 366.

2. Hansen, M., et al., *Assisted reproductive technologies and the risk of birth defects--a systematic review.* Hum Reprod, 2005. **20**(2): p. 328-38.

3. *2008 ART Success Rates Report.* Available from: http://www.cdc.gov/ART.

4. Andersen, A.N., et al., *Assisted reproductive technology in Europe, 2002. Results generated from European registers by ESHRE.* Hum Reprod, 2006. **21**(7): p. 1680-97.

5. *Register of Spanish Society of Infertility: TRA (IA y FIV/ICSI).* . Dynamic Solutions, 2009.

6. Watson, A.J., *The cell biology of blastocyst development.* Mol Reprod Dev, 1992. **33**(4): p. 492-504.

7. Simon, C., et al., *Embryonic regulation in implantation.* Semin Reprod Endocrinol, 1999. **17**(3): p. 267-74.

8. Gardner, D.K., *Textbook of assisted reproductive technologies: laboratory and clinical perspectives.* 3rd ed. 2009, London: Informa Healthcare. xv, 912 p.

9. Lessey, B.A., *Adhesion molecules and implantation.* J Reprod Immunol, 2002. **55**(1-2): p. 101-12.

10. Menezo, Y.J. and D. Sakkas, *Monozygotic twinning: is it related to apoptosis in the embryo?* Hum Reprod, 2002. **17**(1): p. 247-8.

11. Market-Velker, B.A., A.D. Fernandes, and M.R. Mann, *Side-by-side comparison of five commercial media systems in a mouse model: suboptimal in vitro culture interferes with imprint maintenance.* Biol Reprod, 2010. **83**(6): p. 938-50.

12. Horii, T., et al., *Epigenetic differences between embryonic stem cells generated from blastocysts developed in vitro and in vivo.* Cell Reprogram, 2010. **12**(5): p. 551-63.

13. Deng, X., et al., *Effects of different concentrations of amino acids in the culture medium on preimplantation mouse embryo development in vitro.* Di Yi Jun Yi Da Xue Xue Bao, 2005. **25**(3): p. 241-5.

14. Gardner, D.K., et al., *Blastocyst score affects implantation and pregnancy outcome: towards a single blastocyst transfer.* Fertil Steril, 2000. **73**(6): p. 1155-8.

15. Clyde, J.M., et al., *Karyotyping of human metaphase II oocytes by multifluor fluorescence in situ hybridization.* Fertil Steril, 2003. **80**(4): p. 1003-11.

16. Scott, R., et al., *Noninvasive metabolomic profiling of human embryo culture media using Raman spectroscopy predicts embryonic reproductive potential: a prospective blinded pilot study.* Fertil Steril, 2008. **90**(1): p. 77-83.

17. Picton, H.M., et al., *Association between amino acid turnover and chromosome aneuploidy during human preimplantation embryo development in vitro.* Mol Hum Reprod, 2010. **16**(8): p. 557-69.

18. Favetta, L.A., et al., *p66shc, but not p53, is involved in early arrest of in vitro-produced bovine embryos.* Mol Hum Reprod, 2004. **10**(6): p. 383-92.

19. Favetta, L.A., et al., *High levels of p66shc and intracellular ROS in permanently arrested early embryos.* Free Radic Biol Med, 2007. **42**(8): p. 1201-10.

20. Betts, D.H. and P. Madan, *Permanent embryo arrest: molecular and cellular concepts.* Mol Hum Reprod, 2008. **14**(8): p. 445-53.

21. Ebner, T., et al., *Selection based on morphological assessment of oocytes and embryos at different stages of preimplantation development: a review.* Hum Reprod Update, 2003. **9**(3): p. 251-62.

22. Seli, E., C. Robert, and M.A. Sirard, *OMICS in assisted reproduction: possibilities and pitfalls.* Mol Hum Reprod, 2010. **16**(8): p. 513-30.

23. Nagy, Z.P., D. Sakkas, and B. Behr, *Symposium: innovative techniques in human embryo viability assessment. Non-invasive assessment of embryo viability by metabolomic profiling of culture media ('metabolomics').* Reprod Biomed Online, 2008. **17**(4): p. 502-7.

24. Madaschi, C., et al., *Zona pellucida birefringence score and meiotic spindle visualization in relation to embryo development and ICSI outcomes.* Reprod Biomed Online, 2009. **18**(5): p. 681-6.

25. Lopes, A.S., M. Lane, and J.G. Thompson, *Oxygen consumption and ROS production are increased at the time of fertilization and cell cleavage in bovine zygotes.* Hum Reprod, 2010. **25**(11): p. 2762-73.

26. Cruz, M., et al., *Embryo quality, blastocyst and ongoing pregnancy rates in oocyte donation patients whose embryos were monitored by time-lapse imaging.* J Assist Reprod Genet, 2011.

27. Wiener-Megnazi, Z., et al., *Oxidative parameters of embryo culture media may predict treatment outcome in in vitro fertilization: a*

novel applicable tool for improving embryo selection. Fertil Steril, 2011. **95**(3): p. 979-84.

28. Cole, R.J. and J. Paul, *Properties of Cultured Preimplantation Mouse and Rabbitembryos, and Cell Strains Derived from Them*, in *Ciba Foundation Symposium - Preimplantation Stages of Pregnancy*. 2008, John Wiley & Sons, Ltd. p. 82-122.

29. Allen, R.L. and R.W. Wright, Jr., *In vitro development of porcine embryos in coculture with endometrial cell monolayers or culture supernatants.* J Anim Sci, 1984. **59**(6): p. 1657-61.

30. Ellington, J.E., et al., *Bovine 1-2-cell embryo development using a simple medium in three oviduct epithelial cell coculture systems.* Biol Reprod, 1990. **43**(1): p. 97-104.

31. Rubio, C., et al., *Clinical experience employing co-culture of human embryos with autologous human endometrial epithelial cells.* Hum Reprod, 2000. **15 Suppl 6**: p. 31-8.

32. Simon, C., et al., *Coculture of human embryos with autologous human endometrial epithelial cells in patients with implantation failure.* J Clin Endocrinol Metab, 1999. **84**(8): p. 2638-46.

33. Mercader, A., et al., *Clinical experience and perinatal outcome of blastocyst transfer after coculture of human embryos with human endometrial epithelial cells: a 5-year follow-up study.* Fertil Steril, 2003. **80**(5): p. 1162-8.

34. Dominguez, F., et al., *Embryologic outcome and secretome profile of implanted blastocysts obtained after coculture in human endometrial epithelial cells versus the sequential system.* Fertil Steril, 2010. **93**(3): p. 774-782 e1.

35. Baart, E.B., et al., *Milder ovarian stimulation for in-vitro fertilization reduces aneuploidy in the human preimplantation embryo: a randomized controlled trial.* Hum Reprod, 2007. **22**(4): p. 980-8.

36. Sifer, C., et al., *Biological predictive criteria for clinical pregnancy after elective single embryo transfer.* Fertil Steril, 2011. **95**(1): p. 427-30.

37. Carson, D.D., *Embryo implantation : molecular, cellular, and clinical aspects*. 1999, New York: Springer. xviii, 308 p.

38. *Human implantation: recent advances and clinical aspects. Proceedings of and international workshop. Valencia, Spain, 22-23 March 1999.* J Reprod Fertil Suppl, 2000. **55**: p. 1-162.

39. Thie, M., et al., *Cell adhesion to the apical pole of epithelium: a function of cell polarity.* Eur J Cell Biol, 1995. **66**(2): p. 180-91.

40. Varghese, A.C., et al., *Emerging technologies for the molecular study of infertility, and potential clinical applications.* Reprod Biomed Online, 2007. **15**(4): p. 451-6.

41. Korner, J. and R.L. Leibel, *To eat or not to eat - how the gut talks to the brain.* N Engl J Med, 2003. **349**(10): p. 926-8.

42. Gorska, E., et al., *Leptin receptors.* Eur J Med Res, 2010. **15 Suppl 2**: p. 50-4.

43. Mounzih, K., R. Lu, and F.F. Chehab, *Leptin treatment rescues the sterility of genetically obese ob/ob males.* Endocrinology, 1997. **138**(3): p. 1190-3.

44. Cervero, A., et al., *The leptin system during human endometrial receptivity and preimplantation development.* J Clin Endocrinol Metab, 2004. **89**(5): p. 2442-51.

45. Gonzalez, R.R., et al., *Leptin and leptin receptor are expressed in the human endometrium and endometrial leptin secretion is regulated by the human blastocyst.* J Clin Endocrinol Metab, 2000. **85**(12): p. 4883-8.

46. Classen-Linke, I., et al., *The cytokine receptor gp130 and its soluble form are under hormonal control in human endometrium and decidua.* Mol Hum Reprod, 2004. **10**(7): p. 495-504.

47. Stewart, C.L., et al., *Blastocyst implantation depends on maternal expression of leukaemia inhibitory factor.* Nature, 1992. **359**(6390): p. 76-9.

48. Urayama, K., et al., *The prokineticin receptor-1 (GPR73) promotes cardiomyocyte survival and angiogenesis.* FASEB J, 2007. **21**(11): p. 2980-93.

49. Li, M., et al., *Identification of two prokineticin cDNAs: recombinant proteins potently contract gastrointestinal smooth muscle.* Mol Pharmacol, 2001. **59**(4): p. 692-8.

50. LeCouter, J., et al., *The endocrine-gland-derived VEGF homologue Bv8 promotes angiogenesis in the testis: Localization of Bv8 receptors to endothelial cells.* Proc Natl Acad Sci U S A, 2003. **100**(5): p. 2685-90.

51. Soga, T., et al., *Molecular cloning and characterization of prokineticin receptors.* Biochim Biophys Acta, 2002. **1579**(2-3): p. 173-9.

52. Battersby, S., et al., *Expression and regulation of the prokineticins (endocrine gland-derived vascular endothelial growth factor and Bv8) and their receptors in the human endometrium across the menstrual cycle.* J Clin Endocrinol Metab, 2004. **89**(5): p. 2463-9.

53. Hla, T. and K. Neilson, *Human cyclooxygenase-2 cDNA.* Proc Natl Acad Sci U S A, 1992. **89**(16): p. 7384-8.

54. Evans, J., et al., *Prokineticin 1 mediates fetal-maternal dialogue regulating endometrial leukemia inhibitory factor.* FASEB J, 2009. **23**(7): p. 2165-75.

55. Su, M.T., et al., *Polymorphisms of endocrine gland-derived vascular endothelial growth factor gene and its receptor genes are associated with recurrent pregnancy loss.* Hum Reprod, 2010. **25**(11): p. 2923-30.

56. Salker, M., et al., *Natural selection of human embryos: impaired decidualization of endometrium disables embryo-maternal interactions and causes recurrent pregnancy loss.* PLoS One, 2010. **5**(4): p. e10287.

57. Macdonald, L.J., et al., *Prokineticin 1 induces Dickkopf 1 expression and regulates cell proliferation and decidualization in the human endometrium.* Mol Hum Reprod, 2011.

58. Horcajadas, J.A., et al., *Determinants of endometrial receptivity.* Ann N Y Acad Sci, 2004. **1034**: p. 166-75.

59. Kao, L.C., et al., *Global gene profiling in human endometrium during the window of implantation.* Endocrinology, 2002. **143**(6): p. 2119-38.

60. Simon, C. and D. Valbuena, *Embryonic implantation.* Ann Endocrinol (Paris), 1999. **60**(2): p. 134-6.

61. Lessey, B.A., *Two pathways of progesterone action in the human endometrium: implications for implantation and contraception.* Steroids, 2003. **68**(10-13): p. 809-15.

62. Gregory, C.W., et al., *Steroid receptor coactivator expression throughout the menstrual cycle in normal and abnormal endometrium.* J Clin Endocrinol Metab, 2002. **87**(6): p. 2960-6.

63. Bouchard, P., N. Chabbert-Buffet, and B.C. Fauser, *Selective progesterone receptor modulators in reproductive medicine: pharmacology, clinical efficacy and safety.* Fertil Steril, 2011.

64. Bazer, F.W. and O.D. Slayden, *Progesterone-induced gene expression in uterine epithelia: a myth perpetuated by conventional wisdom.* Biol Reprod, 2008. **79**(5): p. 1008-9.

65. Kastner, P., et al., *Two distinct estrogen-regulated promoters generate transcripts encoding the two functionally different human progesterone receptor forms A and B.* EMBO J, 1990. **9**(5): p. 1603-14.

66. Sartorius, C.A., et al., *A third transactivation function (AF3) of human progesterone receptors located in the unique N-terminal*

segment of the B-isoform. Mol Endocrinol, 1994. **8**(10): p. 1347-60.

67. Arnett-Mansfield, R.L., et al., *Subnuclear distribution of progesterone receptors A and B in normal and malignant endometrium.* J Clin Endocrinol Metab, 2004. **89**(3): p. 1429-42.

68. Janne, O., K. Kontula, and R. Vihko, *Progestin receptors in human tissues: concentrations and binding kinetics.* J Steroid Biochem, 1976. **7**(11-12): p. 1061-8.

69. Vegeto, E., et al., *Human progesterone receptor A form is a cell- and promoter-specific repressor of human progesterone receptor B function.* Mol Endocrinol, 1993. **7**(10): p. 1244-55.

70. Mulac-Jericevic, B., et al., *Subgroup of reproductive functions of progesterone mediated by progesterone receptor-B isoform.* Science, 2000. **289**(5485): p. 1751-4.

71. Mulac-Jericevic, B., et al., *Defective mammary gland morphogenesis in mice lacking the progesterone receptor B isoform.* Proc Natl Acad Sci U S A, 2003. **100**(17): p. 9744-9.

72. Mote, P.A., et al., *Colocalization of progesterone receptors A and B by dual immunofluorescent histochemistry in human endometrium during the menstrual cycle.* J Clin Endocrinol Metab, 1999. **84**(8): p. 2963-71.

73. Zhu, Y., et al., *Cloning, expression, and characterization of a membrane progestin receptor and evidence it is an intermediary in meiotic maturation of fish oocytes.* Proc Natl Acad Sci U S A, 2003. **100**(5): p. 2231-6.

74. Zhu, Y., J. Bond, and P. Thomas, *Identification, classification, and partial characterization of genes in humans and other vertebrates homologous to a fish membrane progestin receptor.* Proc Natl Acad Sci U S A, 2003. **100**(5): p. 2237-42.

75. Smith, J.L., et al., *Heterologous expression of human mPRalpha, mPRbeta and mPRgamma in yeast confirms their ability to function as membrane progesterone receptors.* Steroids, 2008. **73**(11): p. 1160-73.

76. Qiu, H.B., et al., *Membrane progestin receptor beta (mPR-beta): a protein related to cumulus expansion that is involved in in vitro maturation of pig cumulus-oocyte complexes.* Steroids, 2008. **73**(14): p. 1416-23.

77. Nutu, M., et al., *Distribution and hormonal regulation of membrane progesterone receptors beta and gamma in ciliated epithelial cells of mouse and human fallopian tubes.* Reprod Biol Endocrinol, 2009. **7**: p. 89.

78. Fernandes, M.S., et al., *Regulated expression of putative membrane progestin receptor homologues in human endometrium and gestational tissues.* J Endocrinol, 2005. **187**(1): p. 89-101.

79. Karteris, E., et al., *Progesterone signaling in human myometrium through two novel membrane G protein-coupled receptors: potential role in functional progesterone withdrawal at term.* Mol Endocrinol, 2006. **20**(7): p. 1519-34.

80. Bartke, A., *Effect of an IUD on implantation and the decidual reaction in different strains of mice.* J Reprod Fertil, 1968. **15**(2): p. 185-90.

81. Mosher, W.D. and W.F. Pratt, *Fecundity and infertility in the United States: incidence and trends.* Fertil Steril, 1991. **56**(2): p. 192-3.

82. Speroff, L. and M.A. Fritz, *Clinical gynecologic endocrinology and infertility*. 7th ed. 2005, Philadelphia: Lippincott Williams & Wilkins. x, 1334 p.

83. Thomsen, R.J. and D.L. Rayl, *Dr. Lippes and his loop. Four decades in perspective.* J Reprod Med, 1999. **44**(10): p. 833-6.

84. Zipper, J., M. Medel, and R. Prager, *Suppression of fertility by intrauterine copper and zinc in rabbits. A new approach to intrauterine contraception.* Am J Obstet Gynecol, 1969. **105**(4): p. 529-34.

85. Holland, M.K. and I.G. White, *Heavy metals and human spermatozoa. III. The toxicity of copper ions for spermatozoa.* Contraception, 1988. **38**(6): p. 685-95.

86. Ammala, M., et al., *Effect of intrauterine contraceptive devices on cytokine messenger ribonucleic acid expression in the human endometrium*. Fertil Steril, 1995. **63**(4): p. 773-8.

87. Gonzalez, R.R., et al., *Abnormal pattern of integrin expression at the implantation window in endometrium from fertile women treated with clomiphene citrate and users of intrauterine device.* Early Pregnancy, 2001. **5**(2): p. 132-43.

88. Tetrault, A.M., et al., *Decreased endometrial HOXA10 expression associated with use of the copper intrauterine device.* Fertil Steril, 2009. **92**(6): p. 1820-4.

89. Horcajadas, J.A., et al., *Effect of an intrauterine device on the gene expression profile of the endometrium.* J Clin Endocrinol Metab, 2006. **91**(8): p. 3199-207.

90. Noyes, R.W., A.T. Hertig, and J. Rock, *Dating the endometrial biopsy.* Am J Obstet Gynecol, 1975. **122**(2): p. 262-3.

91. R Development Core Team. R Foundation for Statistical Computing, V., Austria [ISBN 3-900051-00-3] *A language and environment for statistical computing 2004* 2004; Available from: [**¡Error! Referencia de hipervínculo no válida.**.

92. Dennis, G., Jr., et al., *DAVID: Database for Annotation, Visualization, and Integrated Discovery.* Genome Biol, 2003. **4**(5): p. P3.

93. von Mering, C., et al., *STRING 7--recent developments in the integration and prediction of protein interactions.* Nucleic Acids Res, 2007. **35**(Database issue): p. D358-62.

94. Saeed, A.I., et al., *TM4: a free, open-source system for microarray data management and analysis.* Biotechniques, 2003. **34**(2): p. 374-8.

95. Michael S. Baggish, R.F., Hubert Guedj, *Hysteroscopy: visual perspectives of uterine anatomy, physiology and pathology.* Third Edition ed. 2007.

96. Yokoyama, H., *[Gamma glutamyl transpeptidase (gammaGTP) in the era of metabolic syndrome].* Nihon Arukoru Yakubutsu Igakkai Zasshi, 2007. **42**(3): p. 110-24.

97. Bozza, P.T., et al., *Lipid body function in eicosanoid synthesis: An update.* Prostaglandins Leukot Essent Fatty Acids, 2011.

98. Yaqoob, P., *Fatty acids as gatekeepers of immune cell regulation.* Trends Immunol, 2003. **24**(12): p. 639-45.

99. Wymann, M.P. and R. Schneiter, *Lipid signalling in disease.* Nat Rev Mol Cell Biol, 2008. **9**(2): p. 162-76.

100. Lu, S.C., *Regulation of glutathione synthesis.* Mol Aspects Med, 2009. **30**(1-2): p. 42-59.

101. Lee, S.R., et al., *Increased expression of glutathione by estradiol, tumor necrosis factor-alpha, and interleukin 1-beta in endometrial stromal cells.* Am J Reprod Immunol, 2009. **62**(6): p. 352-6.

102. Mote, P.A., J.D. Graham, and C.L. Clarke, *Progesterone receptor isoforms in normal and malignant breast.* Ernst Schering Found Symp Proc, 2007(1): p. 77-107.

103. Critchley, H.O., et al., *Progestin receptor isoforms and prostaglandin dehydrogenase in the endometrium of women using a levonorgestrel-releasing intrauterine system.* Hum Reprod, 1998. **13**(5): p. 1210-7.

104. Zhu, P., et al., *The effect of a levonorgestrel-releasing intrauterine device on human endometrial oestrogen and progesterone receptors after one year of use.* Hum Reprod, 1999. **14**(4): p. 970-5.

105. Evans, J., et al., *Prokineticin 1 signaling and gene regulation in early human pregnancy.* Endocrinology, 2008. **149**(6): p. 2877-87.

106. Kurita, T., et al., *Stromal progesterone receptors mediate the inhibitory effects of progesterone on estrogen-induced uterine epithelial cell deoxyribonucleic acid synthesis.* Endocrinology, 1998. **139**(11): p. 4708-13.

107. Blockeel, C., et al., *An in vivo culture system for human embryos using an encapsulation technology: a pilot study.* Hum Reprod, 2009. **24**(4): p. 790-6.